1972-09

A study of a severe local storm of 22 April 1971.

Horswell, Charles Edward.

Monterey, California. Naval Postgraduate School

A STUDY OF A SEVERE LOCAL STORM OF 22 APRIL 1971

Charles Edward Horswell

NAVAL POSTGRADUATE SCHOOL
Monterey, California

THESIS

A Study of a Severe Local Storm

of 22 April 1971

by

Charles Edward Horswell

Thesis Advisor: Ronnie L. Alberty

September 1972

A Study of a Severe Local Storm of 22 April 1971

by

Charles Edward Horswell
Lieutenant, United States Navy
B.A., Northwestern University, 1964

Submitted in partial fulfillment of the
requirements for the degree of

MASTER OF SCIENCE IN METEOROLOGY

from the

NAVAL POSTGRADUATE SCHOOL
September 1972

ABSTRACT

A study was made of a severe storm that occurred on 22 April 1971 southeast of Norman, Oklahoma. The life cycle of the storm from origin, through mature stage, to eventual incorporation into a squall line was analyzed. The cell displayed all of the characteristics of a severe local storm, including a hook echo, echo-free vault, sloping overhang, funnel and movement 20° to the right of the mean tropospheric wind. Mesoscale circulations at low and middle levels during the severe stage were revealed by aircraft measured winds. Aircraft meteorological parameter measurements showed the vertical structure and extent of the low-level moist layer. Three-dimensional storm structure at the time a funnel was sighted was inferred from WSR-57 radar antenna tilt sequences and airborne RDR-1 radar RHI profiles.

TABLE OF CONTENTS

LIST OF TABLES

LIST OF ILLUSTRATIONS

LIST OF SYMBOLS AND ABBREVIATIONS

CST - Central Standard Time

DTC - Distance Traveled Count

EMB-1 - Experimental Meteorology Branch program one; a computer program used to process data obtained by an RFF aircraft

IFF - "Identification Friend or Foe;" equipment installed in the aircraft which responds only to an interrogating signal from another radar; used for aircraft identification

NOAA - National Oceanographic and Atmospheric Administration

NM - Nautical mile(s)

NSSL - National Severe Storms Laboratory; one of the environmental research laboratories of NOAA

PPI - Plan Position Indicator

RFF - Research Flight Facility

RHI - Range/height indicator

TACAN - Tactical Air Navigation, UHF navigational radio; provides azimuth and distance information

ACKNOWLEDGEMENTS

The author wishes to express his appreciation to Dr. Ronnie L. Alberty for his guidance throughout the course of this study and his assistance during the preparation of the manuscript.

Special thanks go to Dr. R. L. Elsberry for his helpful comments and recommendations concerning the final draft.

The National Severe Storms Laboratory, Norman, Oklahoma and the Research Flight Facility, Miami, Florida provided the data that made this study possible.

I. INTRODUCTION

Case studies of severe local storms have been used from as early as 1953 to study structure, development and movement. Usually the storms produced damaging tornadoes or hail, which attracted the attention of investigators. It was a study of two storms (Wokingham and Geary), which led Browning and Donaldson (1963) to the conclusion that the severe local storm was a distinct class of local storm. Browning (1964) later designated these SR (S for severe, R for right-moving) storms.

The study of radarscope photographs of this type of storm has been a large factor in gaining an understanding of them. The hook echo, echo-free vault, sloping overhang and motion to the right of the mean tropospheric wind are examples of storm characteristics which were discovered by intensive study of radar photographs of individual storms. Another technique used recently by some investigators has been to plot winds, obtained near a severe storm by an aircraft with a Doppler navigational system, relative to the radar echo centroid of the storm. Studies using this method by Fujita and Grandoso (1968) and Fankhauser (1971) have provided insight into storm-environmental air interaction at middle levels.

The data from ten flights by an instrumented aircraft during the spring storm season in Oklahoma were made available as the result of Project Rough Rider '71. Since the mesoscale network of surface and upper air stations was very limited in 1971, the available data were aircraft winds from the Doppler navigational system, meteorological parameters and radarscope photographs. In addition to aircraft data, surface weather radarscope film was available when a storm was within radar range. One goal of the project was to further investigate any severe local storms

utilizing mesoscale windfields derived from aircraft measured winds and radar photographs from both aircraft and surface weather radars.

On two flights, funnels were sighted by the aircraft crew. On one of these days, April 22nd, the data was fairly complete, consisting of aircraft measured parameters and radar film for the legs the aircraft flew in the vicinity of the storm and complete surface radar coverage throughout the lifetime of the storm. The radar data seemed likely to be interesting since it contained horizontal and vertical sections through a severe storm during a period when a funnel was present. The fact that the airborne and surface radars were in favorable positions for observing this phenomenon made the data somewhat unique. The first objective of the research reported here was to see if the mesoscale windfields from aircraft measured winds fit existing models, and the second was to see if additional insight into the internal flow could be inferred from the radar data.

II. SYNOPTIC SITUATION

A. DATA SOURCE

Analyzed charts by the U.S. Weather Bureau were available for the surface at 0600, 1200 and 1800 CST and for 850-, 700-, 500- and 200 mb at 0600 and 1800 CST for 22 April 1971. Two soundings taken at Tinker Air Force Base, ten miles north of the National Severe Storms Laboratory, Norman, Oklahoma, provided upper air information at 0600 and 1800 CST.

B. SURFACE AND UPPER LEVELS

A surface low near the western end of the Oklahoma Panhandle at 0600 CST (Figure 1) moved eastward during the day and by 1800 CST was situated southwest of Oklahoma City (Figure 2). A north-south orientated, occluded front moved ahead of the low and in the early afternoon thunderstorms developed east of the occluded front and north of the accompanying warm front.

At upper levels the flow was typical of a central plains thunderstorm environment:

1. 850mb - Warm, moist air was being advected northward into Texas and Oklahoma throughout the period (Figures 3 and 4).

2. 700mb - Cool, relatively dry flow from the southwest increased in intensity during the period (Figures 5 and 6).

3. 500mb - A dynamic low moved eastward during the day (Figures 7 and 8). The jet maximum was in optimum position for development at 1800 CST.

4. 200mb - The dynamic low extended to this level (Figures 9 and 10). The jet split during the day with the northerly branch situated

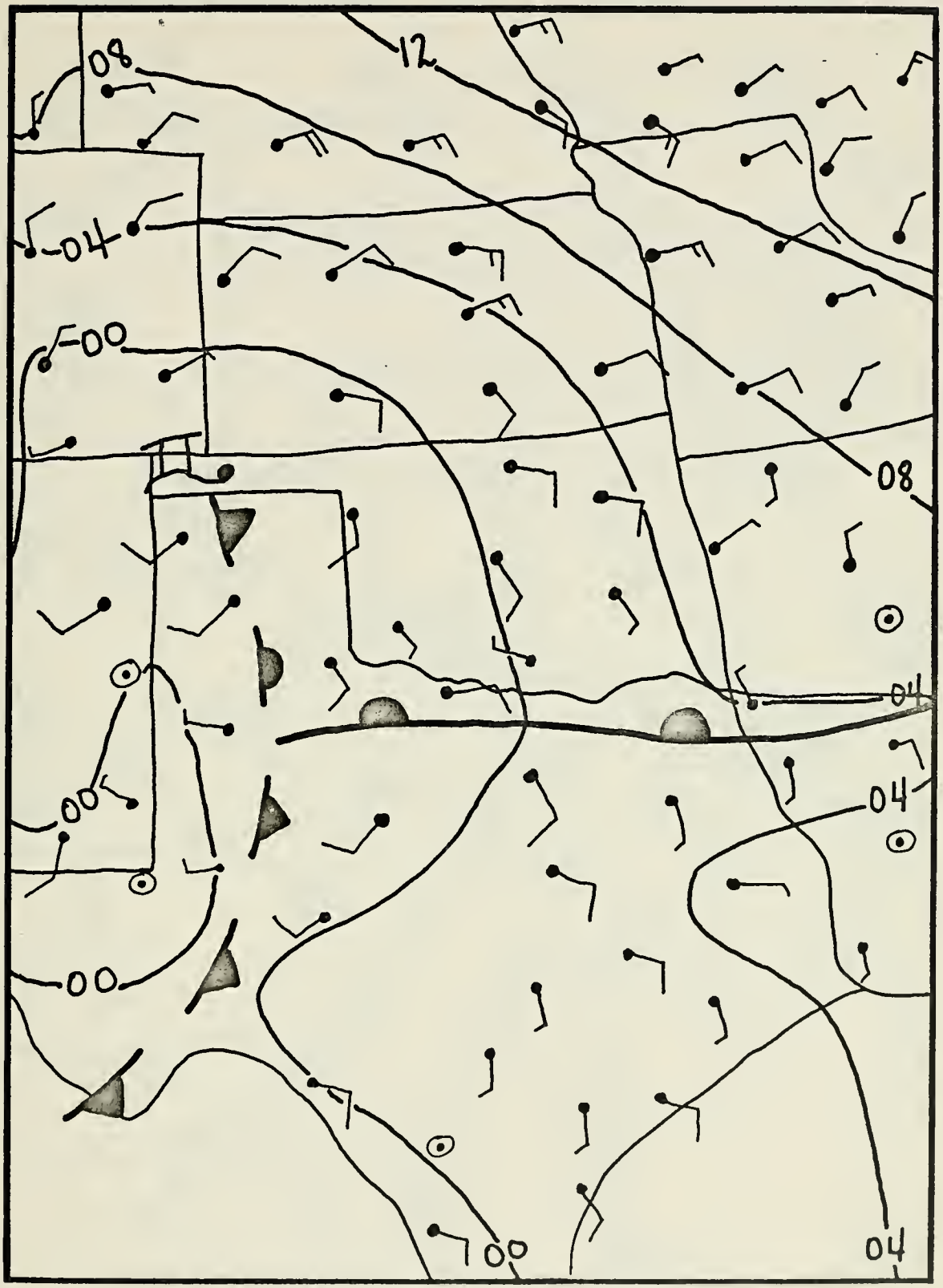

Figure 1. Surface analysis for 0600 CST, 22 April 1971.

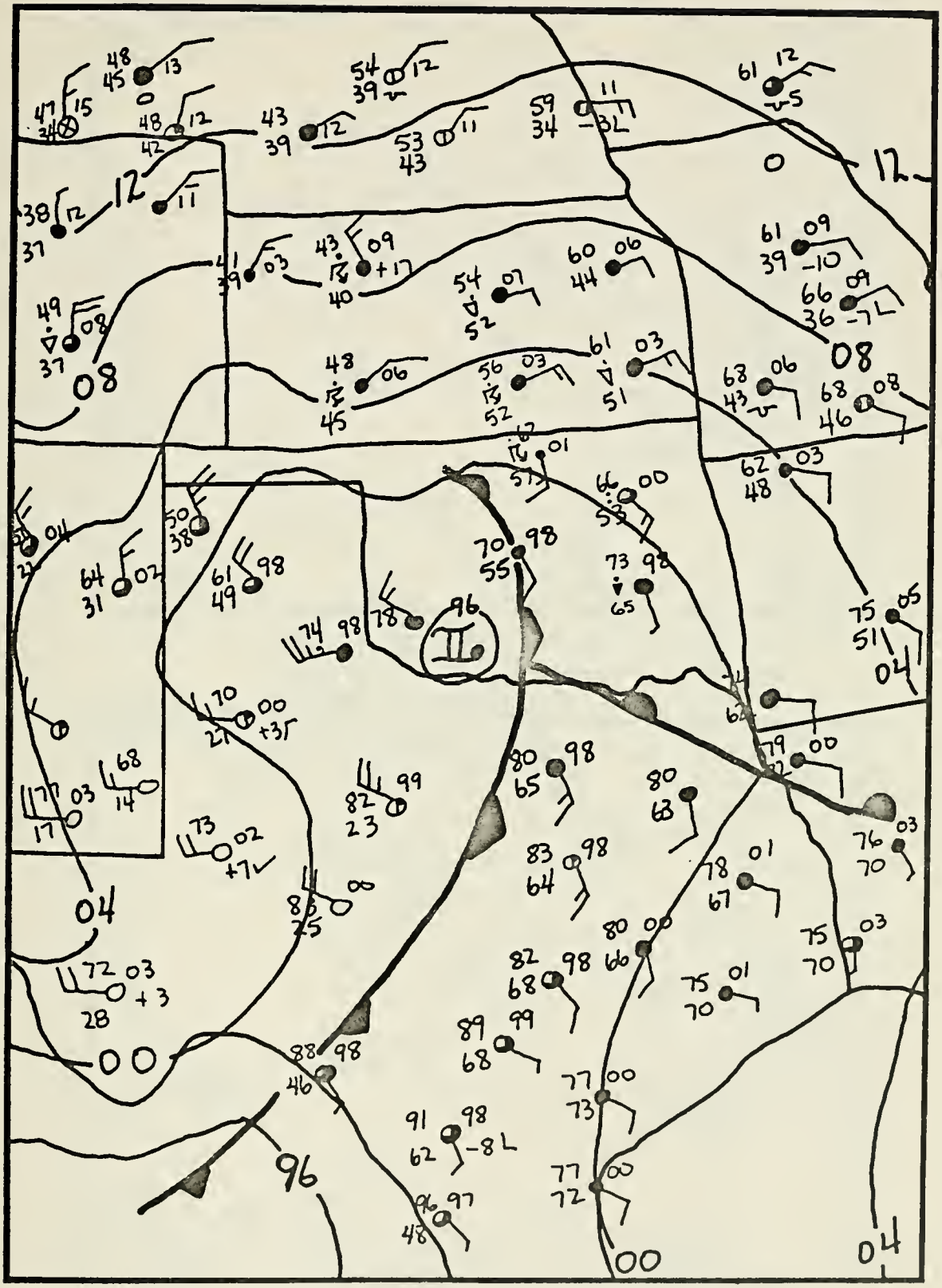

Figure 2. Surface analysis for 1800 CST, 22 April 1971.

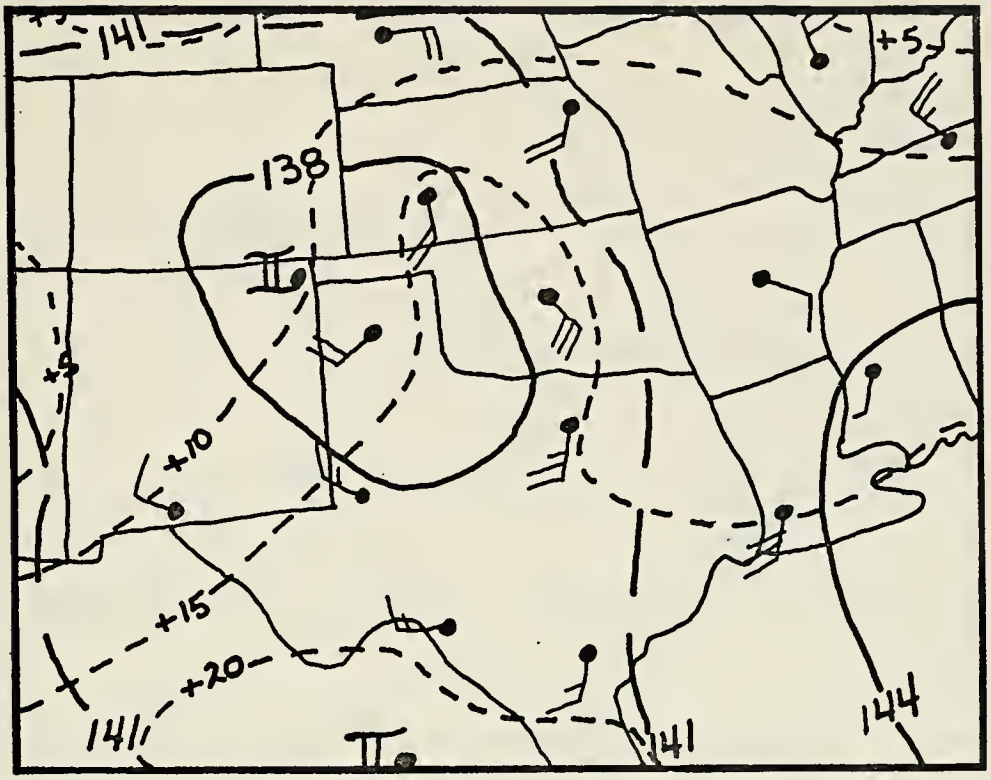

Figure 3. 850mb analysis for 0600 CST, 22 April 1971. Contours are indicated by solid lines and isotherms by dashed lines.

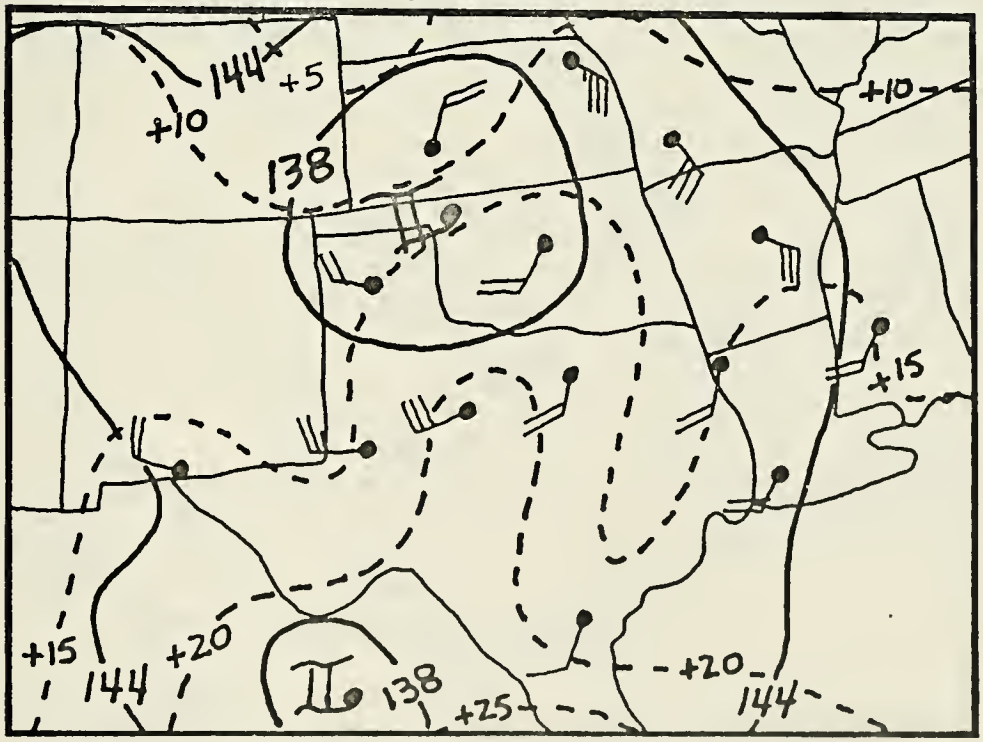

Figure 4. 850mb analysis for 1800 CST, 22 April 1971. Contours are indicated by solid lines and isotherms by dashed lines.

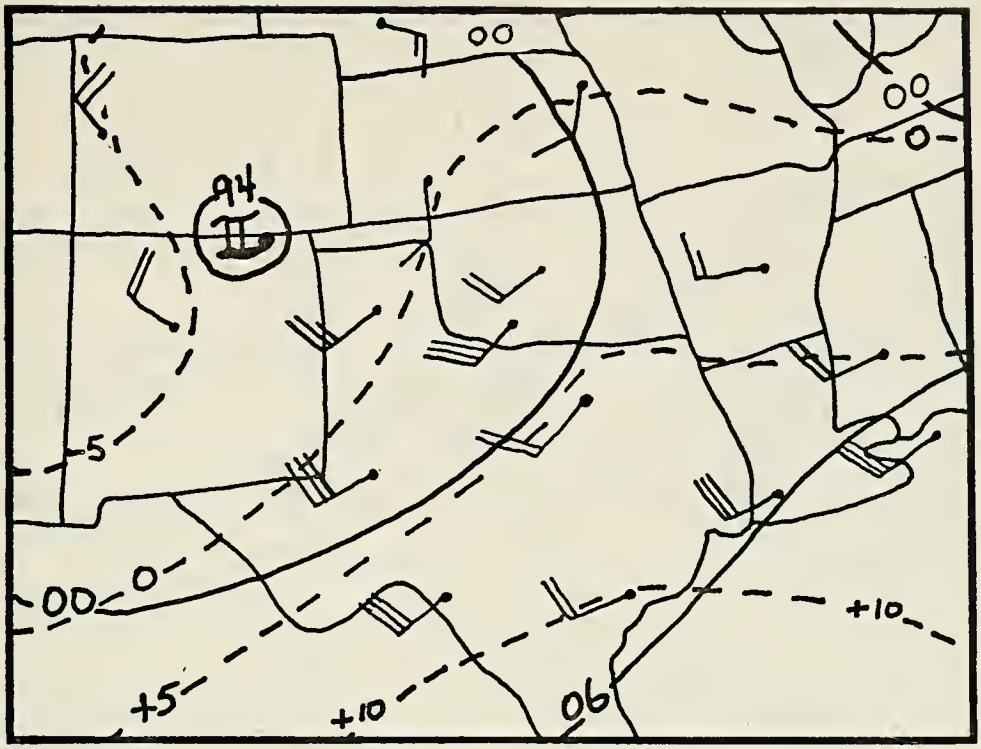

Figure 5. 700mb analysis for 0600 CST, 22 April 1971. Contours are indicated by solid lines and isotherms by dashed lines.

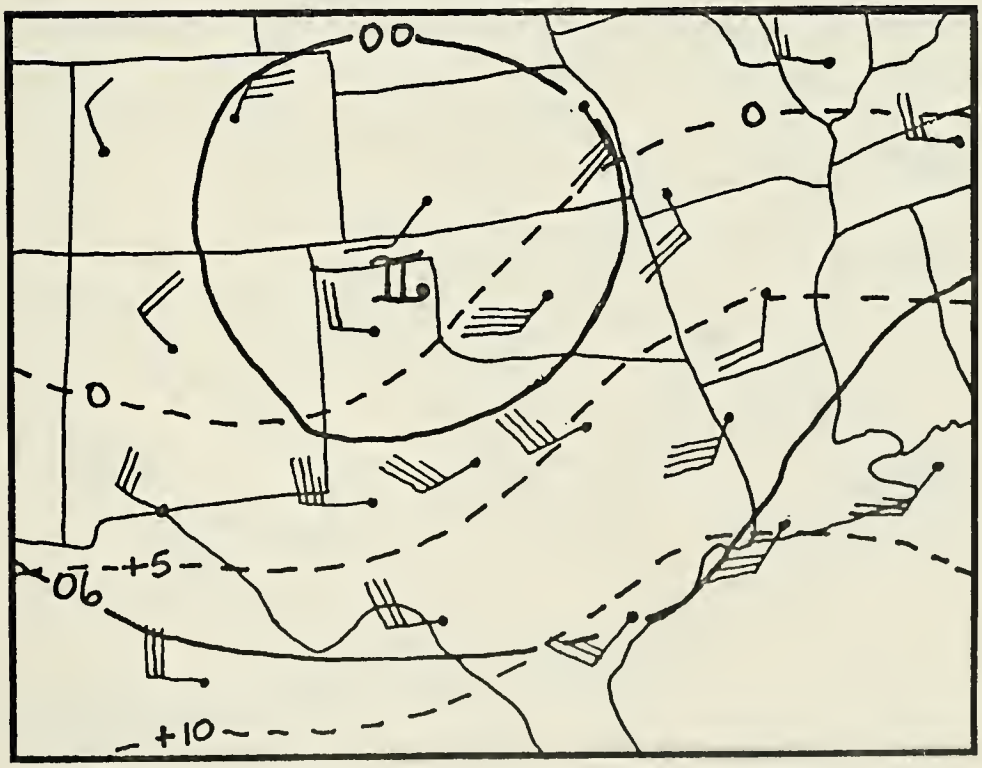

Figure 6. 700mb analysis for 1800 CST, 22 April 1971. Contours are indicated by solid lines and isotherms by dashed lines.

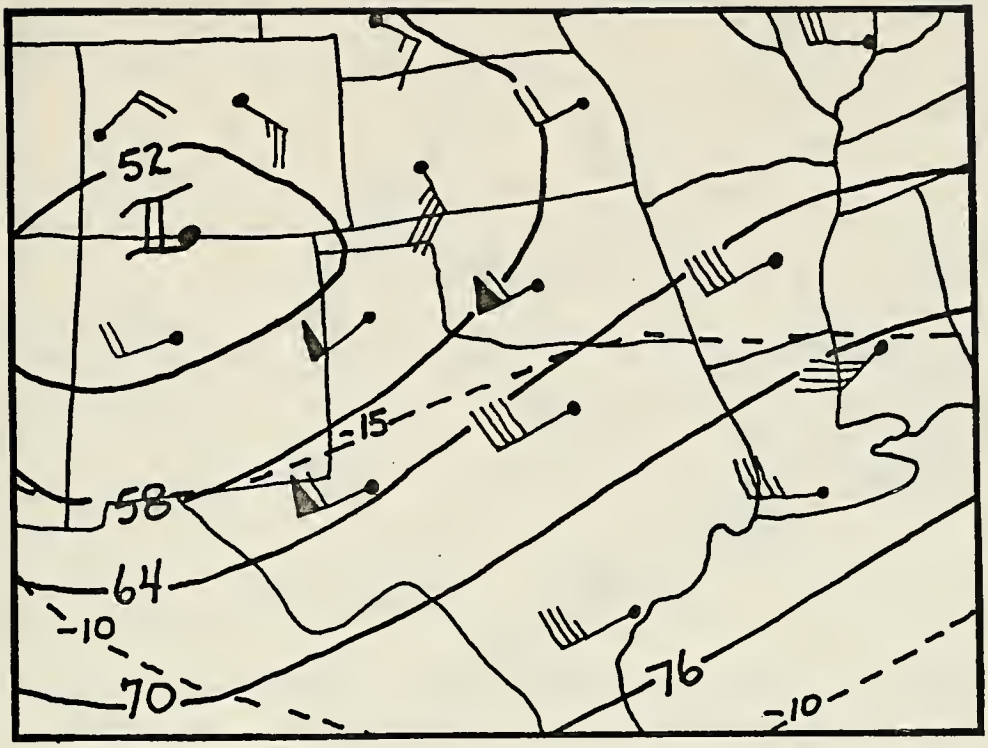

Figure 7. 500mb analysis for 0600 CST, 22 April 1971. Contours are indicated by solid lines and isotherms by dashed lines.

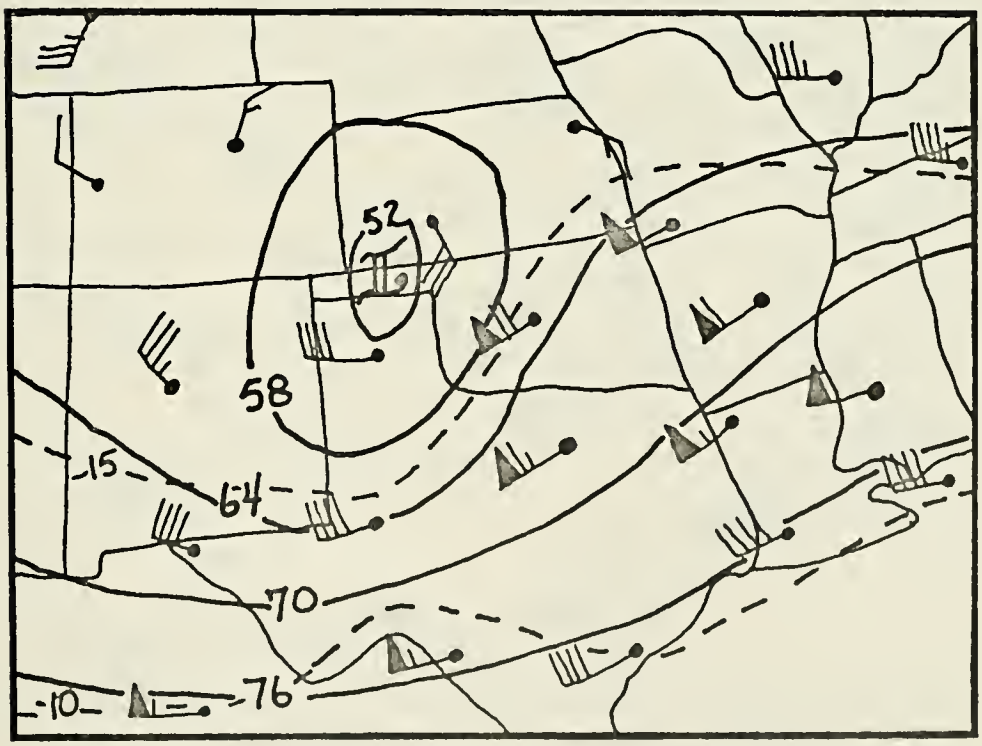

Figure 8. 500mb analysis for 1800 CST, 22 April 1971. Contours are indicated by solid lines and isotherms by dashed lines.

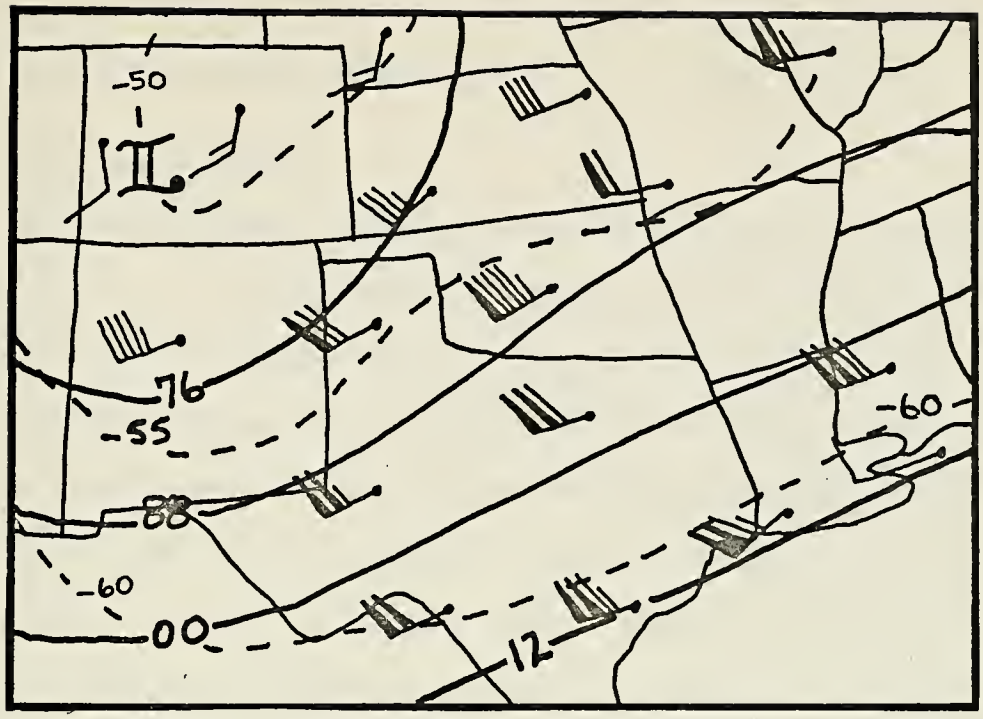

Figure 9. 200mb analysis for 0600 CST, 22 April 1971. Contours are indicated by solid lines and isotherms by dashed lines.

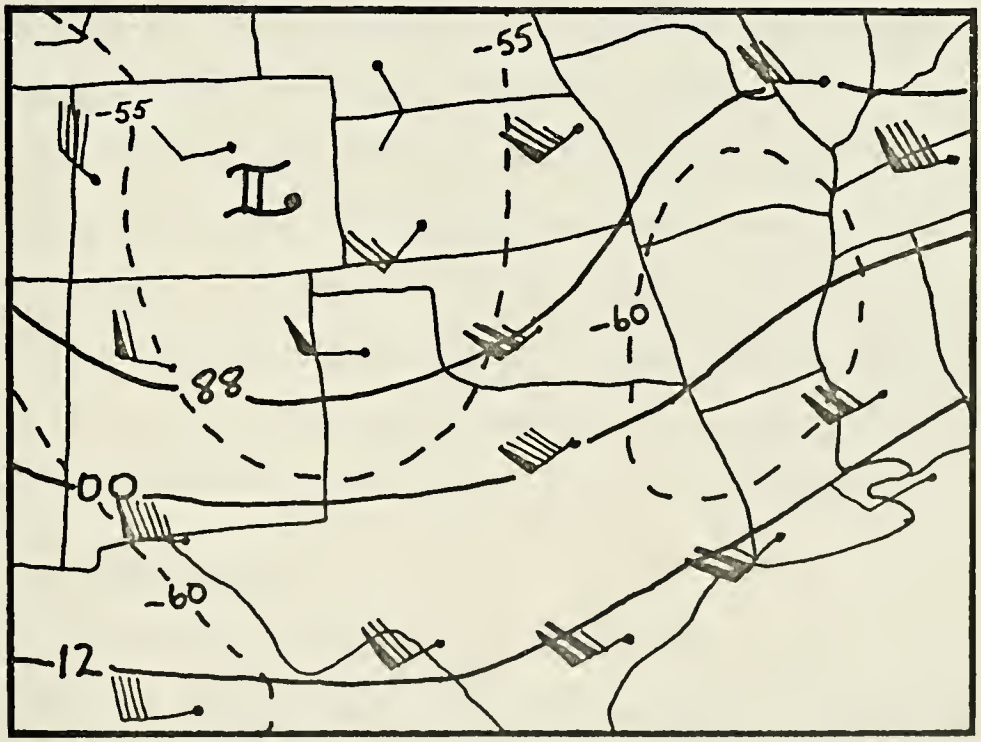

Figure 10. 200mb analysis for 1800 CST, 22 April 1971. Contours are indicated by solid lines and isotherms by dashed lines.

over Oklahoma City at 1800. The -60 °C isotherm moved northward to a position just southeast of the squall line area at 1800 CST.

C. UPPER AIR SOUNDINGS

The 0600 CST Tinker sounding is plotted in skew T-log P coordinates in Figure 11. It had a Showalter Index of +3, due mainly to a low moisture value at 850mb. The lapse rate at midlevels was fairly large and vertical wind shear was strong from 650- to 200mb. The tropopause was at 200mb and the level of maximum winds was slightly higher.

The 1800 CST Tinker sounding is plotted in Figure 12. Between 850-700mb the lapse rate was very large. Low-level moisture had increased during the day as reflected by a Showalter Index of -1. Again the relatively low moisture value at 850mb kept the index low. The tropopause was still at 200mb, but the level of maximum winds was now just below 300mb; a strong jet (136 knots) was present here. Accordingly, the vertical shear between 850- and 300mb was very strong.

Since the 1800 sounding was taken 30 nautical miles northwest of the developing squall line, its indication of the lack of low-level moisture is not believed to be representative of the inflow layer south of the squall line. If the 850mb mixing ratio values recorded southeast of the squall line by the instrumented aircraft, are coupled with the 1800 sounding, a Showalter Index between -5 and -6 is obtained.

D. MEAN TROPOSPHERIC WIND

Fankhauser (1964) computed mean winds using a vector average of 850-, 700-, 500- and 300mb winds. For the 1800 sounding this method yielded a mean tropospheric wind from 230 degrees at 60 knots.

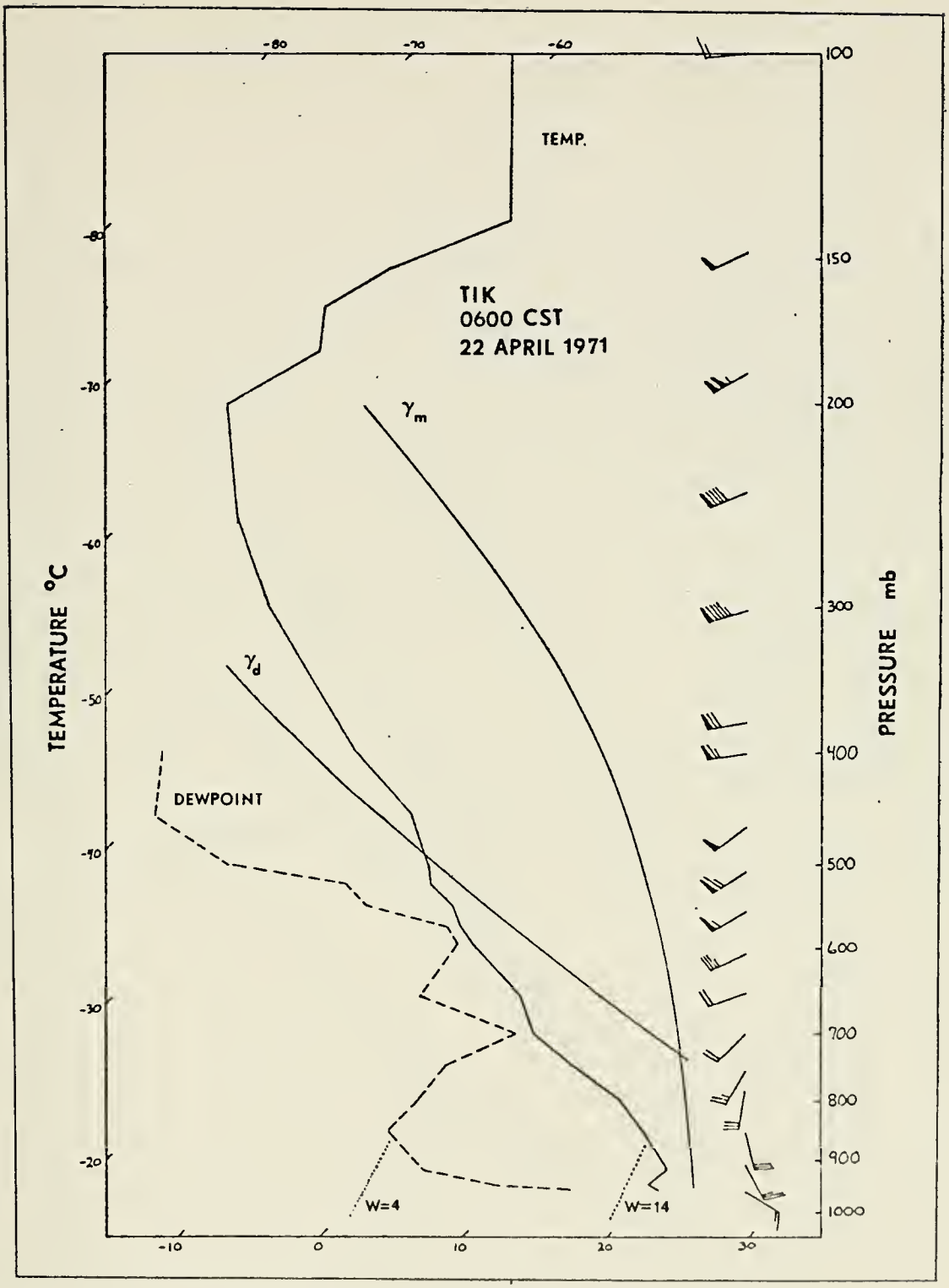

Figure 11. Tinker AFB sounding to 100mb at 0600 CST, 22 April 1971. Temperatures are indicated in degrees Centigrade, pressure in millibars. Sloping dotted lines indicate 4 and 14 gm/kgm mixing ratio coordinates.

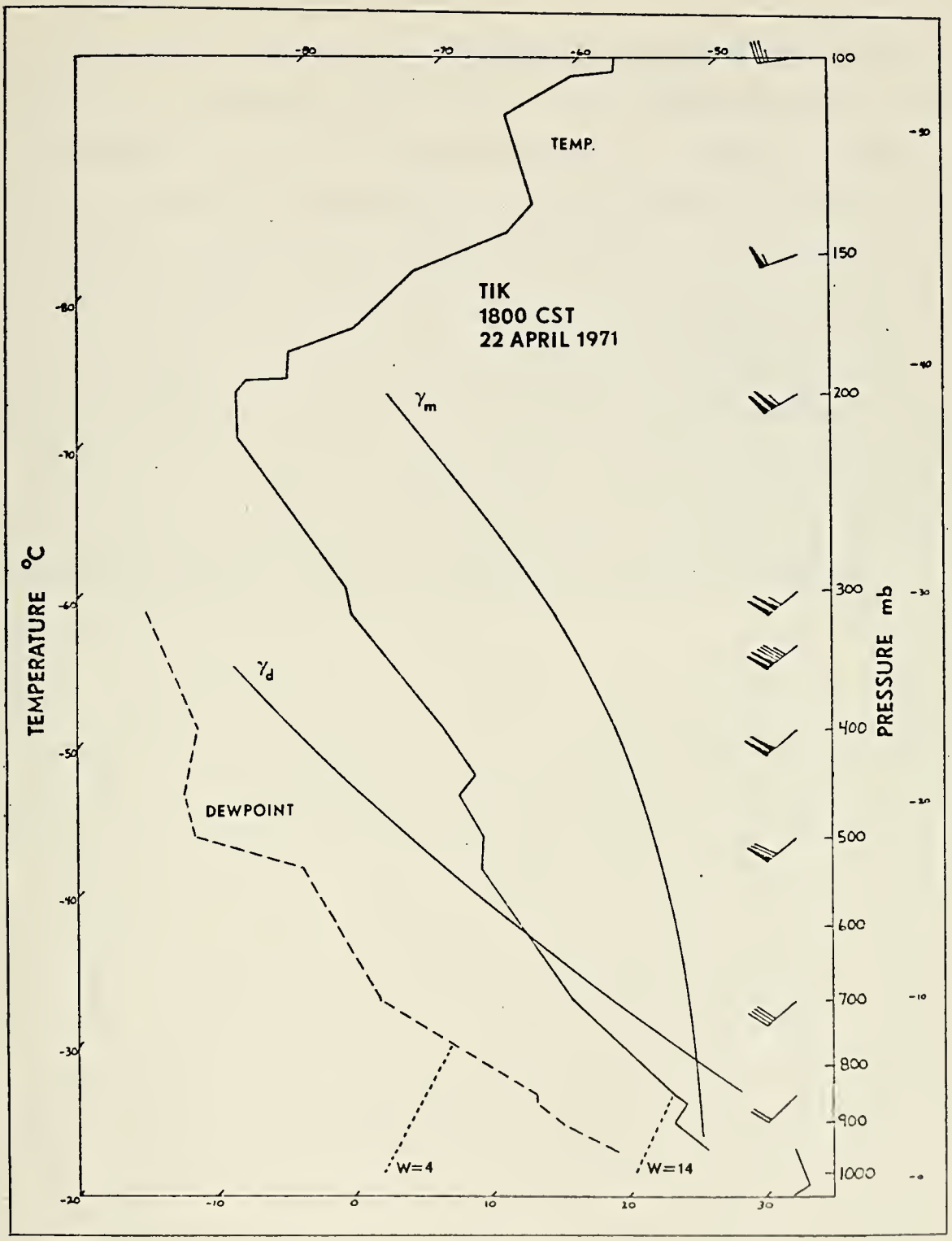

Figure 12. Sounding from Tinker AFB at 1800 CST, 22 April 1971. The squall line was 30 miles southeast of TIK at this time. Temperatures are indicated in degrees Centigrade, pressure in millibars. Sloping dotted lines indicate 4 and 14 gm/kgm mixing ratio coordinates.

E. SUMMARY OF THE SYNOPTIC SITUATION

The severe storm synoptic environment has been discussed by Van Thullenar (Browning and Fujita, 1965). The conditions favorable for the development of severe local storms include (1) a surface low upwind, (2) warm advection at 850mb, (3) a warm ridge upwind at 700mb, (4) a 500mb trough upwind, (5) a high-level jet west or northwest, (6) an unstable atmosphere and (7) the -60 °C isotherm within the general area of development. All of the above conditions except (3) were shown to have been present - (1), (2), (4) and (7) from synoptic analyses and (5) and (6) from the 1800 CST Tinker sounding. Since no storm damage was reported for the 22nd in this area it seems evident that some factors favoring tornado or large hail development were weak or missing.

III. SURFACE WEATHER RADAR ANALYSIS

A. DATA SOURCE

Complete weather radar photographic coverage of the storm from its first appearance on the radarscope until it merged with a developing squall line was made available by the National Severe Storms Laboratory, Norman, Oklahoma. The PPI photographs were taken at the rate of 170 frames per hour. The antenna tilt was kept at 0° except for vertical sequences every ten minutes to show upper-level cell structure and cloud tops. The WSR-57 radar had iso-contouring circuitry so that intensity of cloud reflectivity could be readily discerned. The return was also range normalized.

B. STORM MOVEMENT

Storm movement was plotted by measuring the position of the radar echo centroid relative to the NSSL WSR-57 radar. A position was plotted every ten minutes and resulted in a fairly uniform plot of echo movement as seen in Figure 13.

From the time it first appeared on NSSL's WSR-57 radar, at 1425, until 1530 the developing cell traveled 046° true at an average speed of 25 knots. This was very close to the direction of the mean tropospheric wind from the Tinker sounding taken at 1800 CST. At 1530 the storm veered right 20° to 066° true averaging 25 knots for the next hour and forty minutes. Between 1710 and 1720 the storm turned back to 050° and from 1720 to 1800 averaged 31 knots. After 1800 the storm lost its separate identity when it merged with other cells to the north in a developing squall line.

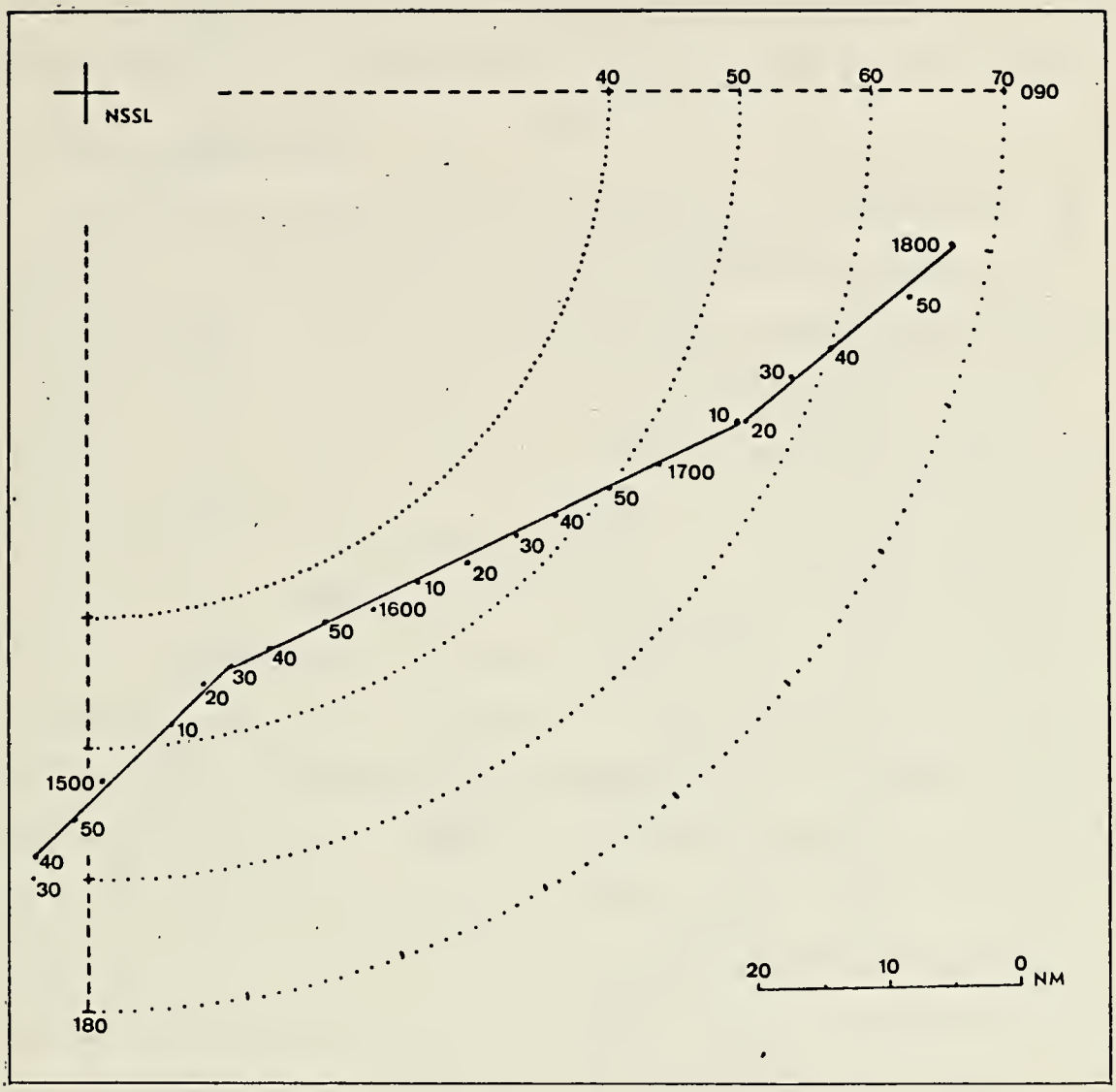

Figure 13. Storm track determined by plotting the range and bearing of the radar echo centroid from NSSL at ten minute intervals. The average direction and speed for each of the three legs were 046/25, 066/25 and 050/31. The mean tropospheric wind at 1800 CST was from 230 at 60 knots.

If the storm being studied and the cell to the north of it at 1430 are followed sequentially in Figure 14, it can be seen that the latter moved northeast at a greater rate. This resulted in the storm merging with the squall line upwind of the cell that was north of it at 1430.

C. STORM DEVELOPMENT

The echo of interest was the southernmost cell at the time it was detected in a north-south line of cells that developed just west of Norman, Oklahoma. Figure 14 shows storm development at ten minute intervals. The first echo appeared at 1425 and five minutes later was eighteen nautical miles long with three cells. Ten minutes after that it had rapidly expanded and was unicellular. The iso-contour feature of the WSR-57 radar showed that echo intensity increased from two contours at 1430 to four at 1437 and gained a fifth at 1445. The long axis of the growing cell can be seen in Figure 14 to have shifted to a more east-west orientation from 1440-1450 and again from 1450-1500 CST. The storm then lengthened between 1500-1510 and rapidly increased in width between 1520-1530. The first finger-like protrusion on the right rear flank appeared at 1508. Hamilton (1969) has previously stated that rapidly developing storms are likely to have severe weather. By 1540 the storm was thirty-two nautical miles long; subsequent growth was small.

At 1530 a definite cyclonic curl can be seen near the upshear end of the cloud (Figure 14) and nine minutes later (at 1539) a hook echo had formed on the right rear flank of the storm. Several of the cells to the north also had pendant echoes extending from their right rear flanks.

At 1600 CST a new cell appeared twenty nautical miles west of the storm under discussion. As can be seen in Figure 14 it developed upwind

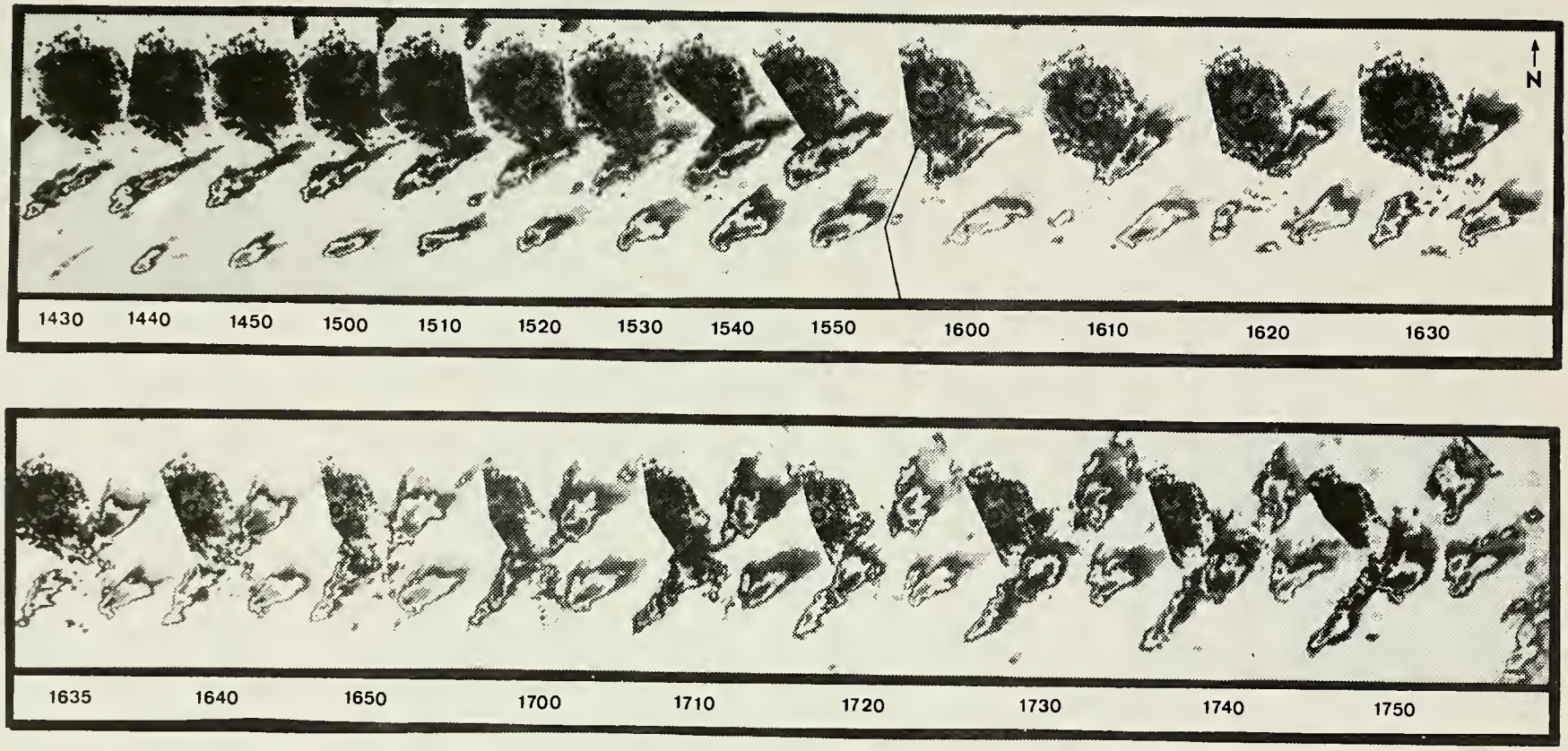

Figure 14. Time-space series of cloud echo photographs at ten minute intervals from the NSSL WSR-57 radar on 22 April 1971. All times are CST and the range marks are spaced every 20 NM. The most southerly cell was the one investigated by the RFF aircraft between 1520 and 1710. Significant features are the hook echo present from 1540-1640 and new cell development at 1600.

of the line of cells to the north. Newton and Fankhauser (1964) have indicated that this is a preferred position for new cell development. In the next few sequences it can be seen that the new cell grew rapidly.

By 1620 CST the hook echo was very pronounced and the shape of the echo closely resembled that of an April 22, 1958 hook echo (Fujita, 1965). The well-developed hook persisted for approximately twenty-five minutes. North of the hook was the area of greatest echo intensity, a characteristic already noted by Fujita (1965) and Kessler (1970).

At 1637 CST the aircraft reported a funnel four to five nautical miles north. Figure 15 shows the aircraft position relative to the storm at that time. By 1644 the hook echo was gone.

The echo was definitely bicellular at 1710 and had increased in size compared with the 1700 echo. Figure 17 shows the storm had reached its maximum horizontal extent at 1710 then rapidly decreased on its downwind left flank between 1710 and 1720; during this period the storm turned to 050, the direction of the mean tropospheric wind. Fankhauser (1971) has pointed out that during a storm's motion to the right of the mean tropospheric wind its precipitation rate increases until just prior to the turnback to the left. He showed a rapid decrease in radar echo area accompanied the turn to the left. By 1750 the storm clearly had become multicellular and within thirty minutes it merged with the developing squall line to the north.

D. VERTICAL CLOUD STRUCTURE NEAR THE TIME OF FUNNEL SIGHTING

The vertical extent of the storm just prior to funnel sighting by the RFF crew is shown in Figure 16(A). The WSR-57 antenna was elevated successively through 0, 1, 2, 4, 6, 8 and 10 degrees of elevation beginning at 1630.3 CST. The hook is clearly visible at 0 and 1 degrees of

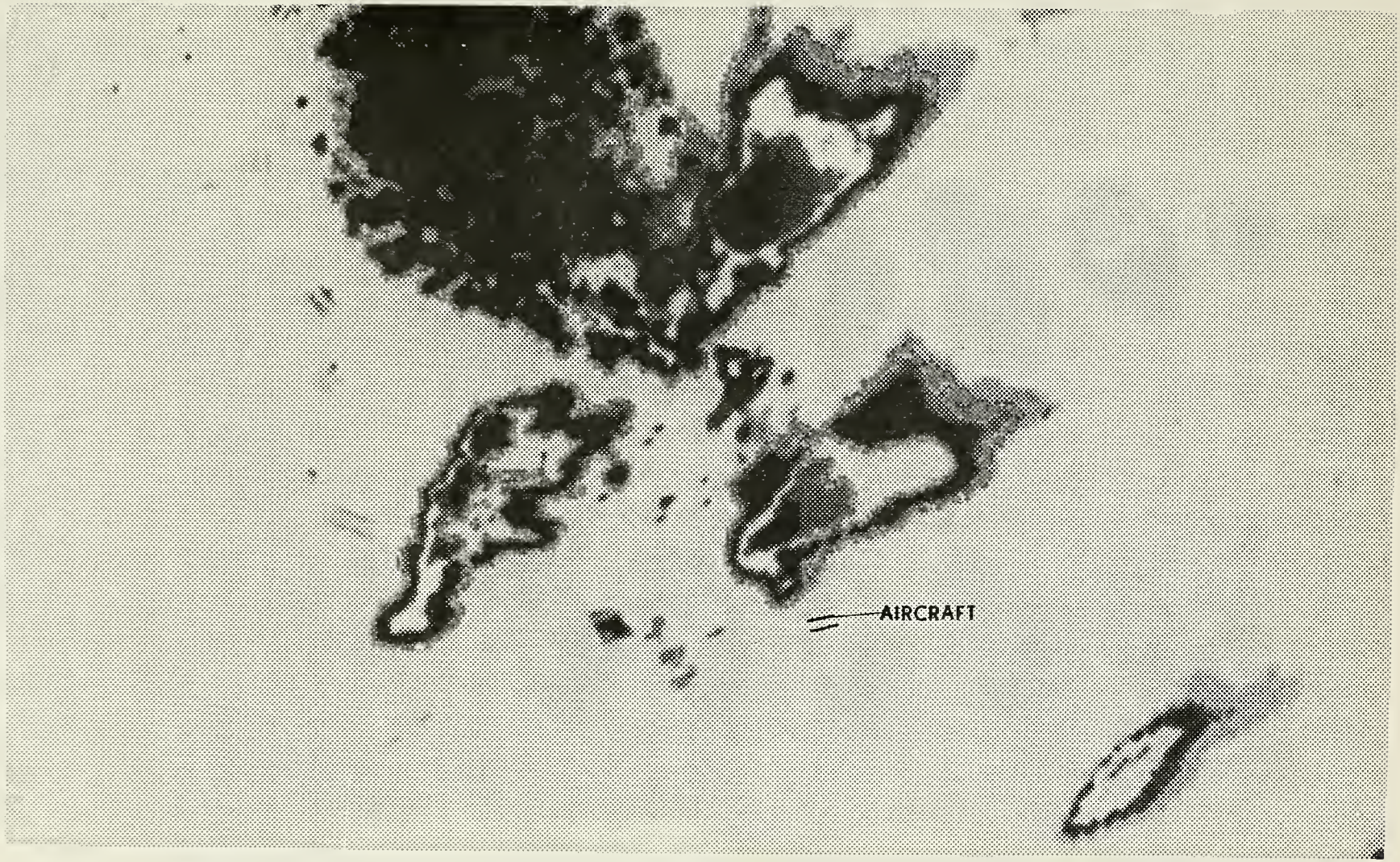

Figure 15. WSR-57 radarscope photograph at 1637 CST, 22 April 1971, the time a funnel was sighted 4-5NM north of the aircraft by the crew. Aircraft IFF return is shown to the south of the hook echo.

Figure 16. WSR-57 antenna tilt sequences of a severe storm near the time a funnel was sighted.
(A) Sequence from 1630.3 to 1632.4 CST, 5 minutes prior to the time of funnel sighting. Cloud tops extended to 50,500 feet. Note apparent vortex at 2^{o} with corresponding curvatures at 1^{o} and 4^{o}.
(B) Sequence from 1640.4 to 1642.2 CST, 3 minutes after funnel sighting. Cloud tops had decreased from previous sequence.

elevation but not at higher elevations. It has been noted by Fujita (1965) that the hook may disappear when antenna elevation angle is increased, implying a tilting of the axis of circulation. Hamilton (1969) reported that the hook may be found at high (25,000 feet) or low levels.

At 2° tilt the highly reflective portion of the echo is seen to have formed what appears to be a cyclonic vortex. The most intense return at 4° tilt also had a corresponding curvature. South of the apparent vortex at 2° tilt were two spots, which were interpreted to have a lesser reflectivity than surrounding areas. A spot was also present at 1° tilt in the center of the hook region immediately under the westernmost spot at 2° tilt.

The cellular nature of the upper portion of the cloud was evident at 6° and 8° of tilt as seen in Figure 16(A). The highest radar echo was directly above the notch observed at lower elevation, a characteristic noted by Browning and Donaldson (1963). The last echo from the storm was at 10° tilt, which corresponded to a height of 50,500 feet or about 10,000 feet above the tropopause level. Donaldson (1965) has pointed out that storms whose tops exceed the tropopause by 10,000 feet will be severe with a tornado likely. It was shortly after this sequence that the funnel was sighted.

Three minutes after the aircraft sighted the funnel at 1637 CST another antenna tilt sequence commenced at 1640.4. In Figure 16(B) a well-defined hook can be seen at 0° but no longer at 1° tilt. The sequence further reveals that the apparent vortex viewed at 2° tilt was gone and the area of intense reflectivity at 2°, 4°, and 6° tilt decreased. By comparing upper cloud levels in Figures 16(A) and 16(B) it can easily be seen that the cloud just before funnel sighting was more symmetric

and extended to higher levels. Here 8° tilt corresponded to approximately 41,500 feet. It may be recalled that the hook echo present at 0° tilt was gone by 1644 CST.

E. SUMMARY OF THE SURFACE RADAR ANALYSIS

The analysis of the WSR-57 radarscope photographs has revealed that this storm (1) moved to the right of the mean tropospheric wind, (2) displayed a hook echo at low-levels on the PPI, (3) had an echo top that extended more than 10,000 feet above the tropopause, (4) had high radar reflectivity (five iso-contours) throughout most of its life and (6) appeared to have a region of cyclonic rotation near the center of its upshear end. The above list included nearly all of the radar characteristics of a severe local storm or SR storm, missing only the persistent echo-free vault. Hamilton (1969) has reported that very few vaults have been observed with the WSR-57 radar, due possibly to its 2° beam width. The presence of the above characteristics coupled with the sighting of a funnel leave little doubt that this storm reached the severe stage of development.

IV. ANALYSIS OF AIRCRAFT MEASURED MESOSCALE WINDS

A. DATA SOURCE

Aircraft data in the form of meteorological parameters and navigational information recorded on magnetic tape at one second intervals, navigational logs and flight summaries were made available by the NOAA Research Flight Facility (RFF), Miami, Florida. The aircraft was an instrumented DC-6B operating under the control of NSSL personnel who followed the storm on surface weather radar as the aircraft gathered data.

B. NAVIGATION

The EMB-1 program (Friedman et al., 1969) was used to reconstruct the aircraft track. The portion of the track in the vicinity of the storm, beginning at 1506 and ending at 1746 CST, was broken into seven legs. Each leg began with a fix to prevent track errors from accumulating. Five of the fixes came from the flight navigational log and were all TACAN. The need for additional fix information to break up legs with excessive end-of-leg errors was partially met by generating radar fixes from aircraft IFF and skin "paints" on the WSR-57 radarscope film. Two such fixes (at 1626 and 1640) came from radar film. Several radar/TACAN fix comparisons were made to see if they were compatible; they agreed to within a mile. The objective was to correct navigation to within one nautical mile, which is the maximum error Fujita (1963) quotes as allowable for mesoscale wind analyses. Table I lists the errors for the legs. The largest end-of-leg error was two nautical miles with most legs having errors of less than one nautical mile. Further WSR-57 radar fixes of aircraft position were not obtainable during the two legs with greater

than one nautical mile errors because the aircraft was over the radar horizon for most of each leg.

Table I. The accumulated error at the end of each leg after track reconstruction by the EMB-1 program.

LEG	TIME (CST)	ERROR (NM)	TYPE FIX
1	1506-1558:40	0.8	TACAN
2	1558:40-1619	0.58	TACAN
3	1619-1626	0.64	Radar
4	1626-1640	1.81	Radar
5	1640-1709	2.07	TACAN
6	1709-1719	0.68	TACAN
7	1719-1744	1.0	Radar

In addition to the navigational accuracy problem, a further correction had to be made to the distance traveled count (DTC) as recorded on the CONVT tape (Friedman et al., 1969). The DTC counter had malfunctioned causing the count to advance only as far as 320 then jump back to 300 throughout the flight. This error had to be corrected before the track could be reconstructed by the EMB-1 program, since the program uses DTC as the basis of the reconstruction.

C. MESOSCALE CIRCULATION AT TWO LEVELS

To show the mesoscale circulation near the storm, a plot was made of the aircraft position relative to the radar echo centroid at one minute intervals. The wind direction and speed from the EMB-1 program were

plotted at each position in the form of a wind barb. This method was similar to that used by Fankhauser (1971). Winds were averaged over a 60 second interval, and the storm was assumed to be steady-state for the averaging interval.

Flow in the vicinity of the storm at the 750mb level is depicted in Figure 17. The following results were noted:

1. There appears to have been a slightly diverging flow around the upwind end of the storm.

2. The winds at this level seem to fit the Browning (1964) model, which has middle-level air entering a severe storm on its right flank ahead of the updraft region. The Fankhauser (1971) model also has middle-level air entering a severe storm in this region, but at a level higher than 750mb.

3. The storm track was definitely to the right of these winds.

After completion of the 750mb legs the aircraft descended to cloud base level (1500-2000 feet) and flew several legs back and forth along the southern flank of the storm. Figure 18 shows aircraft positions plotted relative to the radar echo centroid at one minute intervals with aircraft measured winds at each position shown by the wind barbs. Inflow of warm (18-20 ^{o}C), moist (mixing ratio of 13-14 gm/kgm) air was present all along the southern flank. It has been pointed out by Browning (1964) and Fankhauser (1971) that the right forward flank is the preferred region for updraft entry into the severe type of storm that moves to the right of the mean tropospheric wind.

On two occasions, when the aircraft descended from 750- to 900mb and when it departed the vicinity of the storm, the vertical wind structure could be examined. Figure 19 shows how the wind backed as the aircraft

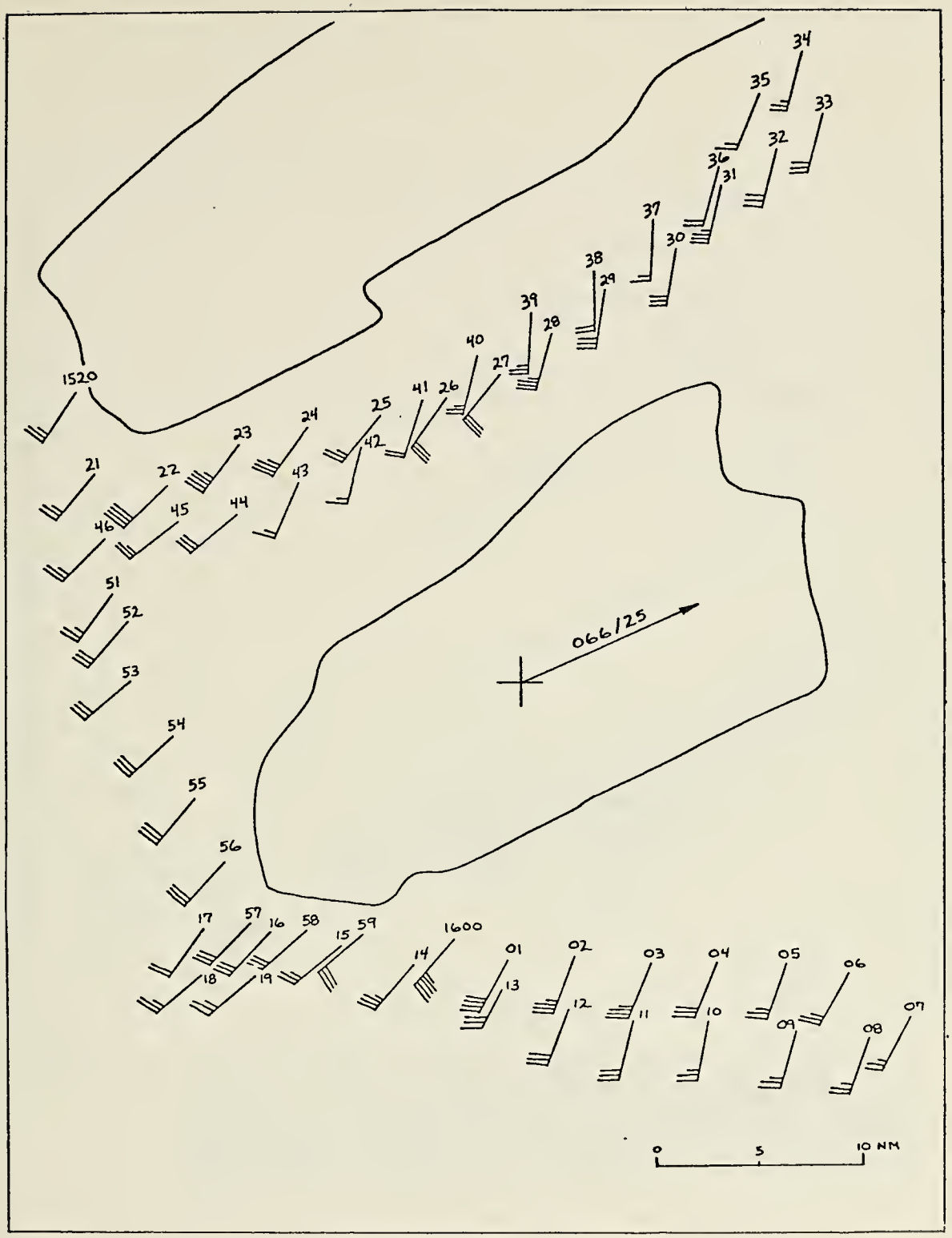

Figure 17. Aircraft flight track relative to radar echo centroid (+) with aircraft measured winds shown plotted at one minute intervals along the track. From 1520 to 1620 CST the aircraft altitude was predominantly at the 750mb level. The radar echo shapes are from 1550 CST.

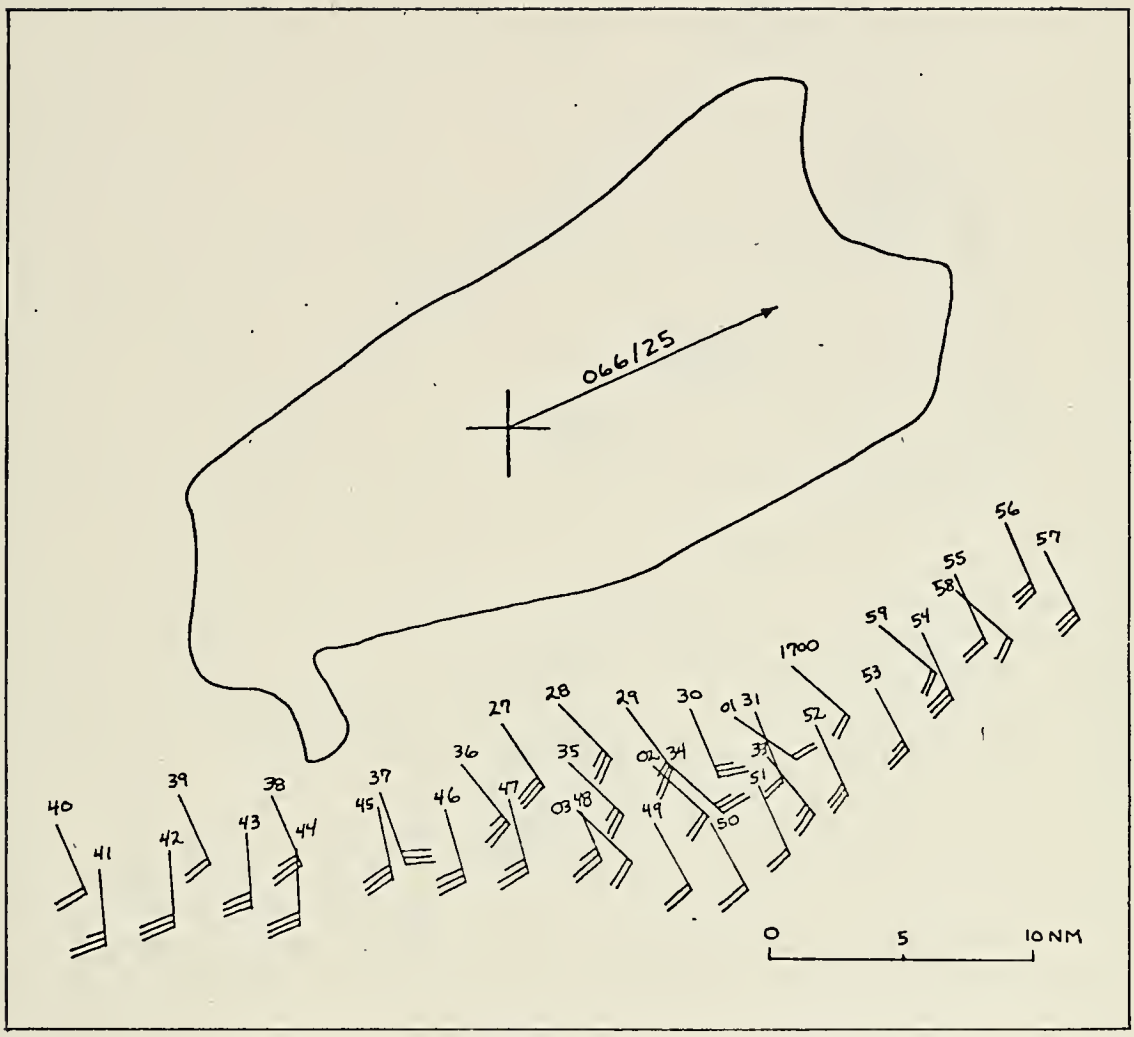

Figure 18. Aircraft flight track relative to radar echo centroid (+) from 1627 to 1703 CST with aircraft measured winds shown plotted at one minute intervals along the track. Aircraft pressure measurements varied from 889- to 921mb during this period. The echo shape is that of the storm at 1635 CST.

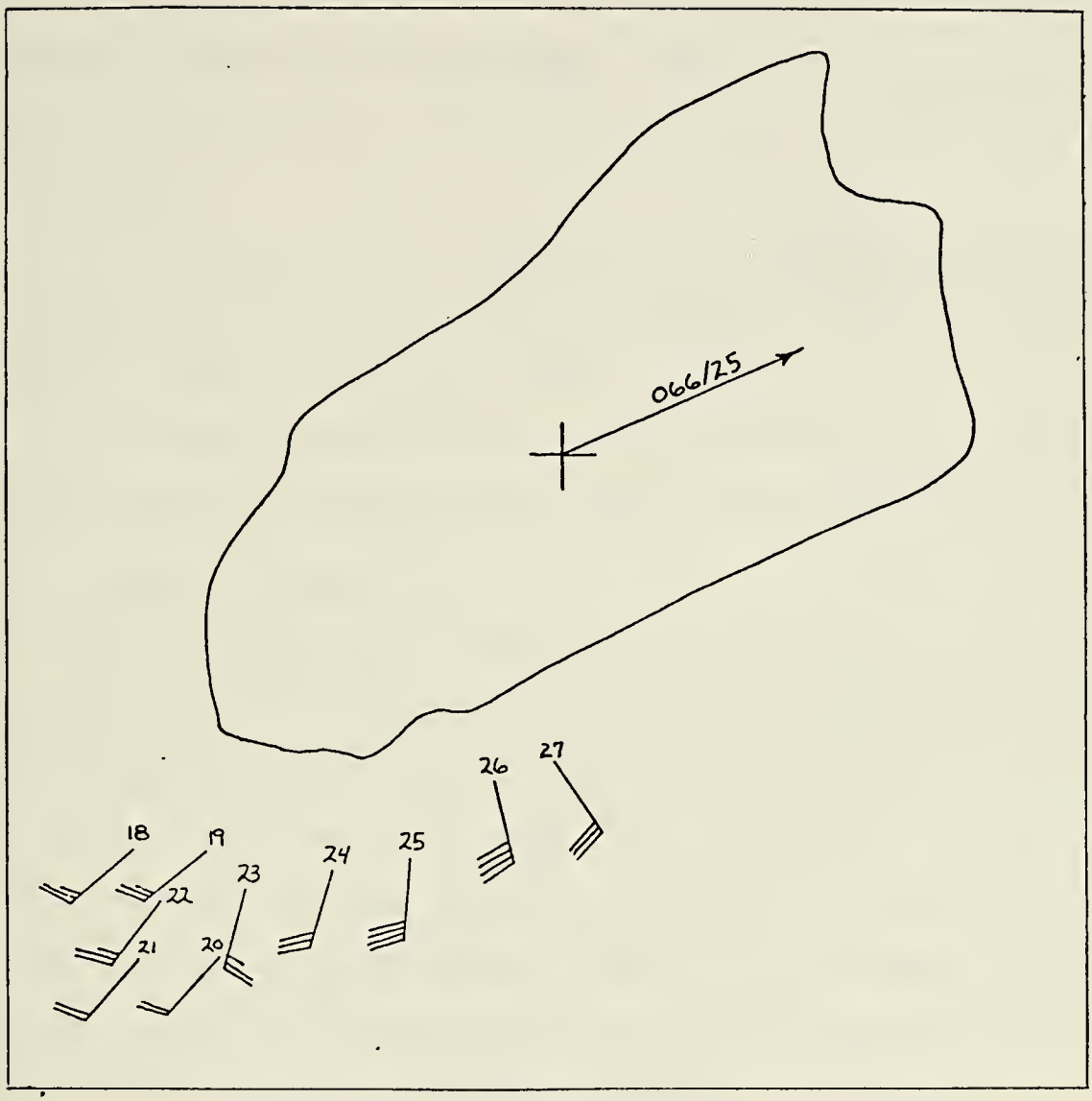

Figure 19. Aircraft flight track relative to radar echo centroid (+) with aircraft measured winds shown plotted at one minute intervals along the track. The aircraft descended from the 750mb level at 1618 to the 890mb level at 1626 CST.

descended from 750- to 890mb. Table II gives pressure, temperature, wind and moisture values at one minute intervals during descent. Figure 20 shows how the wind veered as the aircraft ascended when it departed the area of the storm after the last low-level leg. Table III lists important meteorological parameters measured by the aircraft during this increase in altitude. The study of these profiles led to the following conclusions:

1. The change in wind direction between the surface and upper levels occurred below 750mb. Above 750mb little change in direction occurred but the vertical shear was very large.

2. The moist layer extended to the 850- to 800mb level. A fairly sharp drop in the moisture value at 800mb is shown in Table III.

D. SUMMARY OF AIRCRAFT DATA

The two mesoscale windfields substantiate existing models as to the location of low-level inflow of warm, moist air and middle-level inflow of cooler, drier air. Aircraft wind measurements during the two significant altitude changes showed veering with height to the 750mb level. Above this level the wind speed increased markedly with height but the direction remained fairly constant. Mixing ratio and relative humidity values recorded at the same time showed the vertical extent of the low-level moist layer was between 850- and 800mb.

Table II. Important parameters measured by the RFF aircraft during descent to cloud base level.

TIME (CST)	PRESSURE (mb)	RADAR ALT (feet)	TEMP (°C)	M/R (gm/kgm)	RH %	WIND (knots)
1618	755	6610	7.4	6.7	77	231/25
1619	772	6114	9.0	8.1	85	232/26
1620	802	5196	11.7	8.1	74	223/22
1621	827	4262	13.5	9.5	79	223/22
1622	842	3648	14.6	10.7	84	207/25
1623	864	3171	15.7	12.2	91	196/27
1624	875	2928	16.8	11.7	83	198/33
1625	880	2655	16.4	13.0	95	185/38
1626	890	2128	16.9	13.7	99	165/38
1627	889	2111	16.6	13.7	100	146/31

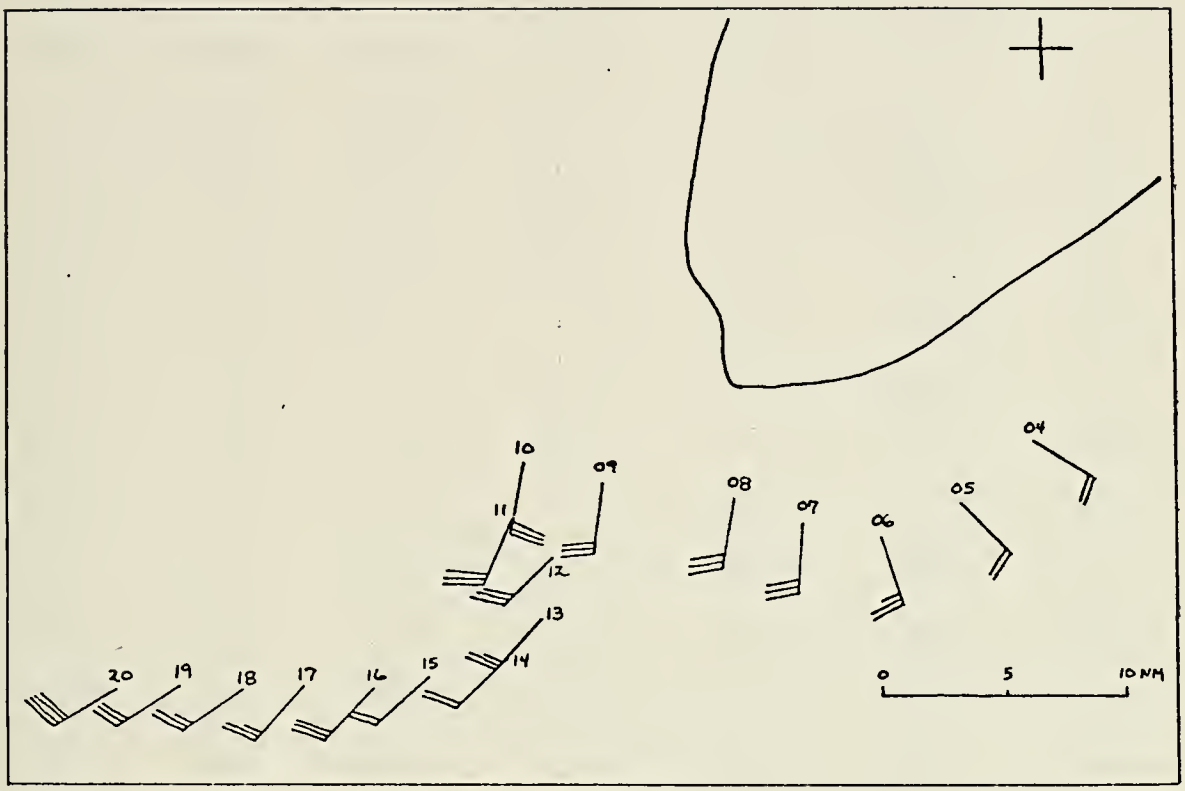

Figure 20. Aircraft flight track relative to radar echo centroid (+) with aircraft measured winds shown plotted at one minute intervals along the track. The veering of the wind with height is shown as the aircraft gained altitude between 1704 and 1720 CST when departing the storm. The echo shape is that of the storm at 1710 CST.

Table III. Important parameters measured by the RFF aircraft during ascent upon departing the vicinity of the storm.

TIME (CST)	PRESSURE (mb)	RADAR ALT (feet)	TEMP (°C)	M/R (g/kg)	RH %	WIND (knots)
1704	921	1276	17.9	13.8	96	122/19
1705	909	1673	17.3	13.9	99	137/19
1706	895	2053	17.0	13.4	96	162/26
1707	866	2935	15.2	12.9	100	183/29
1708	847	3514	14.8	11.0	86	190/31
1709	825	4227	12.6	10.5	92	187/32
1710	805	4919	11.2	10.9	103	191/31
1711	789	5491	10.2	7.9	78	203/28
1712	770	6168	9.2	6.8	70	227/28
1713	751	6933	7.6	6.0	68	230/24
1714	735	7505	5.8	6.1	76	220/24
1715	722	8118	4.2	6.5	89	227/22
1716	709	8625	4.0	4.6	62	222/30
1717	686	9608	1.6	4.8	76	223/26
1718	667	10020	-0.5	4.0	72	235/25
1719	658	10349	-1.9	3.7	72	238/32
1720	634	11293	-4.0	3.3	72	239/39

V. AIRCRAFT RADAR DATA ANALYSIS

A. DATA SOURCE

WP-101 and RDR-1 radarscope film was made available by the NOAA Research Flight Facility (RFF), Miami, Florida. Each exposure of the 35mm film rolls had an annotation consisting of time, radar type, range scale and photo number. The overall picture quality was excellent.

B. WP-101 RADAR DATA

The WP-101 is a forward looking, 5cm radar with a PPI presentation capable of displaying echoes within 120° to the right or left of aircraft heading. Radarscope photographs in Figure 21 show how the hook echo appeared on 5cm radar at 1558, 1614, 1623 and 1637 CST, the latter being at the time of the funnel sighting. The respective aircraft levels were 753-, 752-, 863- and 904mb. The hook echo and echo-free vault can be seen to be very well-formed at 1637. The hook at 1637 was fairly wide and was associated with a funnel, which tends to support Hamilton's (1969) statement that a large diffuse hook may be associated with a funnel aloft.

C. RDR-1 RADAR DATA

The RDR-1, a 3cm radar with a 360° scope presentation, has its antenna mounted perpendicular to the longitudinal axis of the aircraft to give a RHI profile of clouds on both sides of the aircraft (Reber and Friedman, 1964). The radar has an iso-echo feature which shows regions of high reflectivity by blanking out the return from that portion of the cloud. The areas of intense reflectivity can be discerned from noncloudy areas because the former are completely surrounded by weaker echo. The optimum range for this radar is from 5-12 nautical miles (P. Black, NHRL, personal

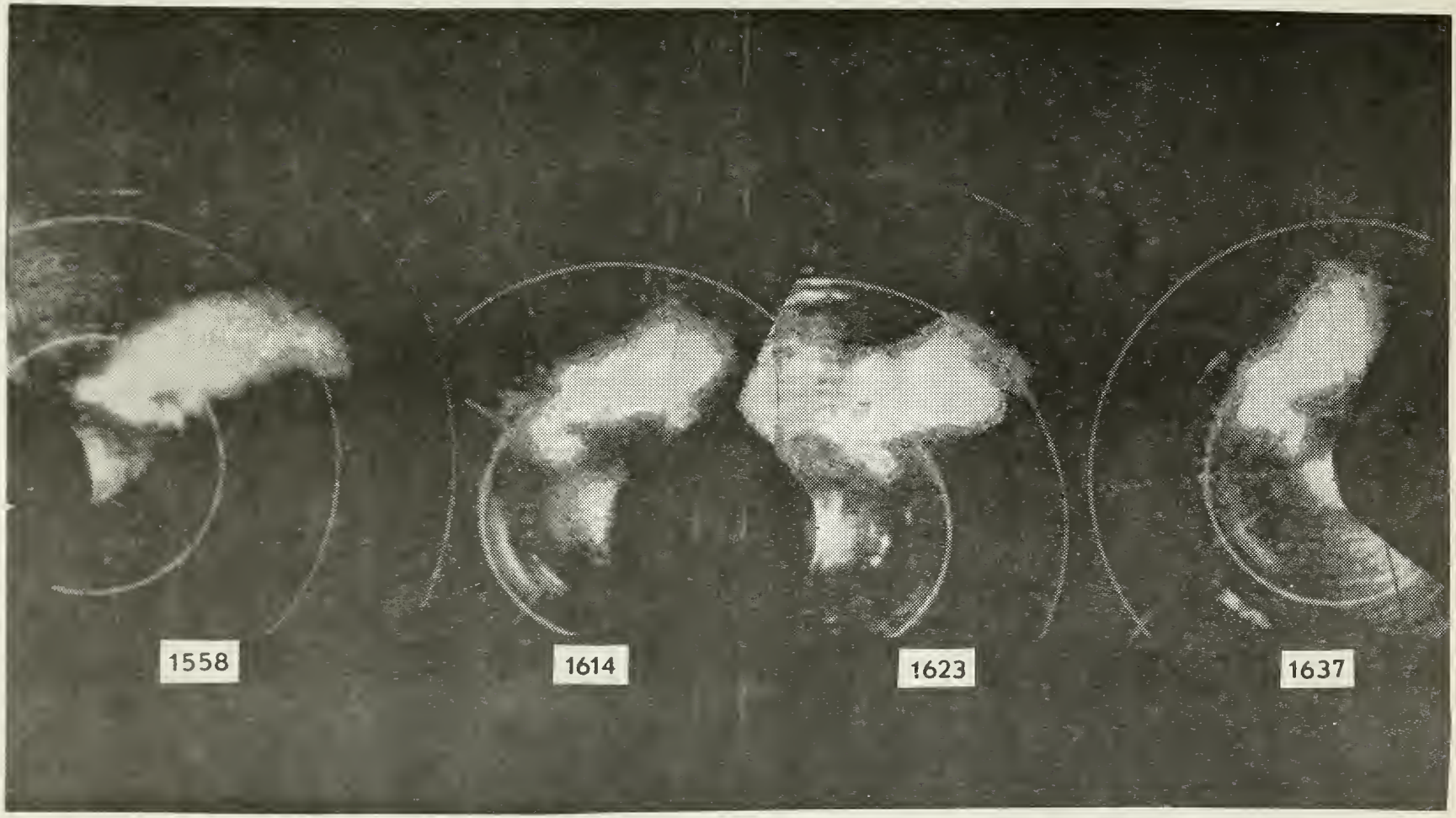

Figure 21. Hook echo development as shown by the airborne WP-101 radar. 1637 CST was the time a funnel was sighted by the aircraft crew. The range marks are every 10 NM.

correspondence). This wavelength of radar is back-scattered by almost all cloudy matter. An advantage of the scope presentation of this radar is that it doesn't distort the image by horizontal compression; a feature common to most RHI profiles. There may, however, be echo attenuation on the side of the storm away from the aircraft due to the short wavelength of this radar.

Radarscope photographs from two legs flown at cloud base level, parallel to the long axis of the storm, were studied. The photographic sequences show vertical profiles of the storm, nearly perpendicular to its longitudinal axis, approximately every nautical mile.

The first leg beginning at 1626 CST, was flown on a heading that varied from 080-094 true and at ground speeds from 158-201 knots. Basically the aircraft flew east along the southern flank of the storm. Figure 22 shows the vertical profiles numbered in sequential order. The following features were present:

1. As the aircraft passed the upshear end of the storm, the radarscope camera recorded an intensely reflective return (the hook) and, north of that, the echo-free vault.

2. The next six profiles show the vault extending up through the cloud, a region of overhang south of the vault and a large, intensely reflective streamer extending from high levels on the southern flank of the storm.

3. In profiles 3-8, an intensely reflective portion of the storm north of the vault at low and middle levels can be seen.

4. In profiles 9 and 10, a sloping overhang formed the southern flank of the storm at low to middle levels. The vertical extent of the storm as determined by radar return was close to 60,000 feet (Reber and Friedman, 1964).

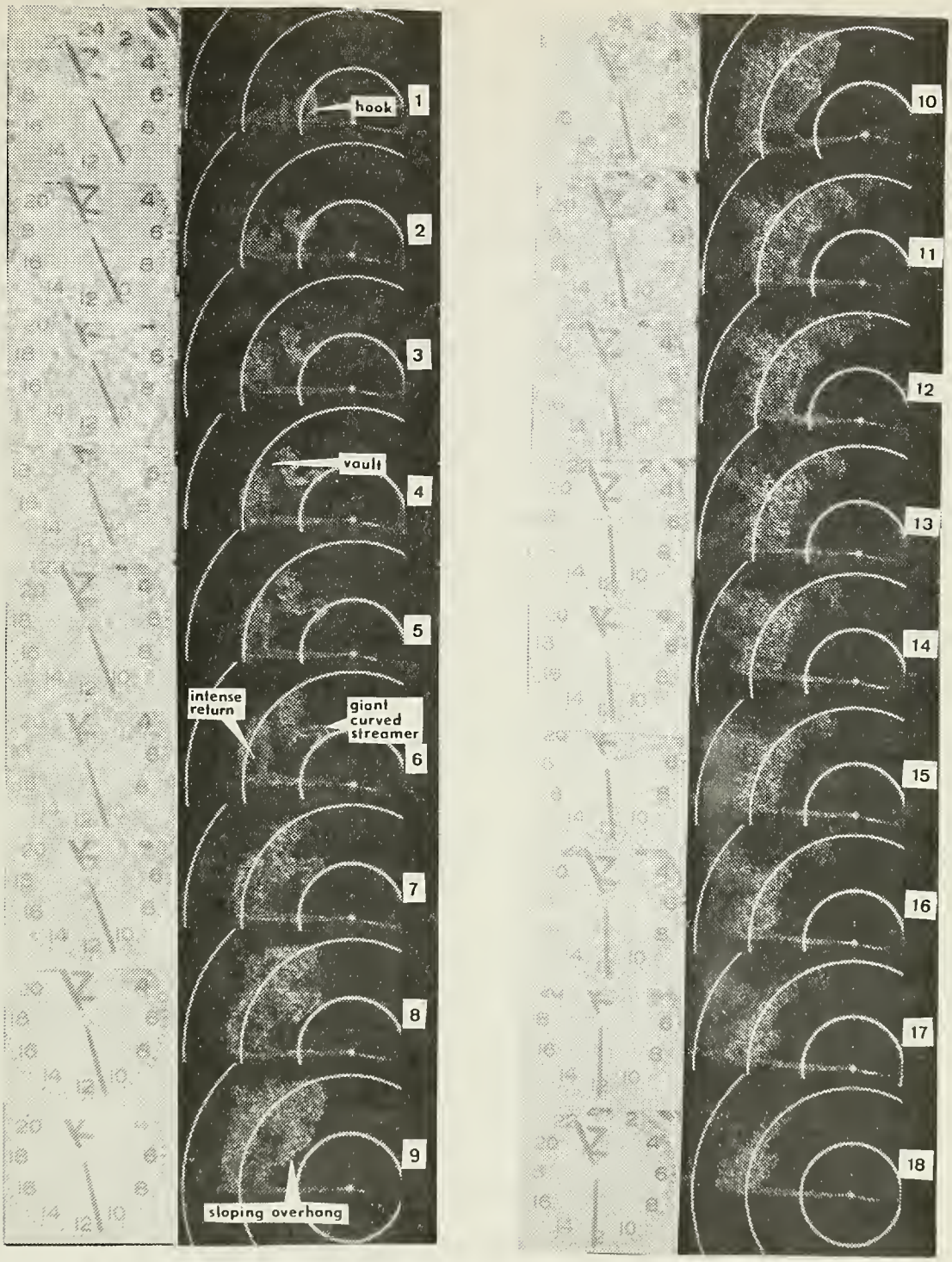

Figure 22. RHI profiles perpendicular to the long axis of the storm from airborne RDR-1 3cm radar. The sequence began at 1626 and ended at 1630 CST. Profiles are numbered consecutively. The aircraft position is the center of the concentric range circles which are spaced every 5NM.

5. The remaining profiles show the forward portion of the storm.

The second leg was the opposite of the first in that the aircraft flew west along the southern flank of the storm. The sequence began at 1634.6 and ended at 1638.7. It was during this period that the funnel was sighted by the crew. A heading of 260 true was maintained and the ground speed varied from 204-212 knots. A careful examination of the sequence of RHI profiles in Figure 23 revealed the following details:

1. Overall, the storm profiles (Figure 23) are considerably different from those of the previous leg (Figure 22).

2. Profiles 1 and 2 show the forward portion of the storm decreased in vertical extent compared to the earlier leg.

3. Profiles 2-10 show an intensely reflective area (dark portion in the center of the profile due to the iso-echo feature) at middle levels extended from near the southern flank of the storm back to the center of the cell in the rear of the storm.

4. In profiles 5-10 the sloping overhang is seen to have been lower and more pronounced than earlier.

5. Profiles 8-14 show vertical cross-sections through the hook echo region. If one views these profiles in reverse order, the hook observed in 14 appears at successively lower levels proceeding forward to 9.

6. Starting with profile 9, an echo-free area appears between the hook and the overhang above it. The echo-free region can be followed section by section back through the storm. This region has been named the vault by Browning (1964) and is adjacent to the core of the updraft, where vertical velocities exceed the fall speed of precipitation particles. Profile 11 shows the vault occupied the center of the cloud profile and was surrounded by intensely reflective echo. Browning and Ludlam

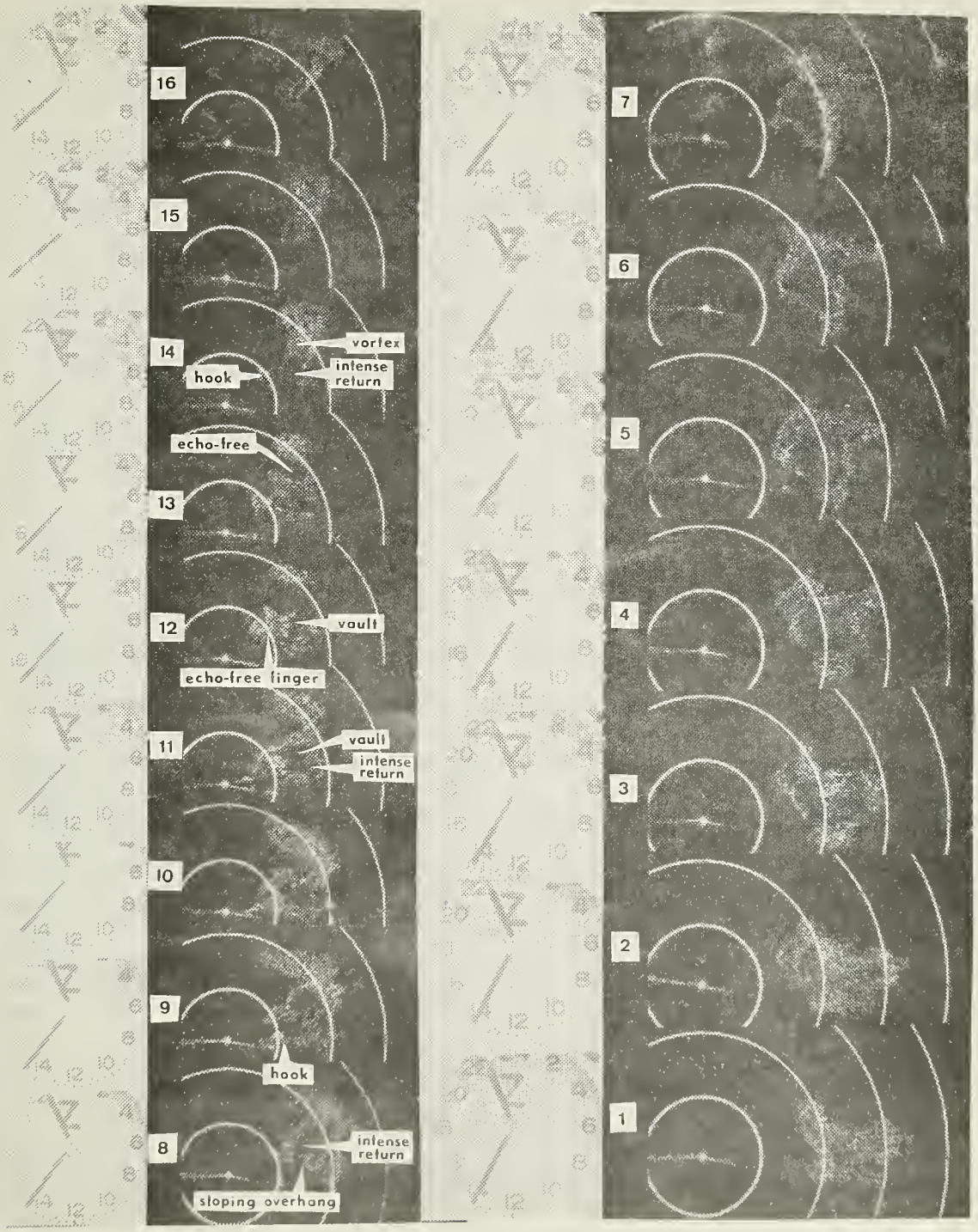

Figure 23. RHI profiles perpendicular to the long axis of the storm from airborne RDR-1 3cm radar. The sequence began at 1634 and ended at 1639 CST. Profiles are numbered consecutively. The aircraft position is the center of the concentric range circles which are spaced every 5NM.

(1962) described the vault as tilting toward the rear and left side of the storm with height, which can be seen in profiles 9-12.

7. Profiles 12 and 13 show there was an echo-free region between the upper and lower portion of the storm. The following profile (14) reveals a horizontally-oriented vortex that was located just upshear of the echo-free region. Figure 24 is an enlarged view of 14. Beneath this vortex was an intensely reflective region, which extended south of the storm forming the upshear edge of the hook echo.

8. The cloud bases and tops extend to higher levels proceeding upwind (profiles 12-16). The cloud tops appear to have reached the 60,000 foot level in the upshear end of the storm.

9. A possible region of entry of the funnel into the storm is shown by profiles 10, 11 and 12 in the center of the hook. This position corresponds well with the reported position of the funnel, four to five nautical miles north of the aircraft. Profile 12 further shows an echo-free "finger" angled toward the vault. Assuming that Bates' "flanking line" corresponds to the hook echo region, profile 12 is similar to his depiction of funnel entry into the updraft if only one funnel were present (Severe Storms Research Group of Saint Louis University, 1970).

D. SUMMARY OF AIRCRAFT RADAR ANALYSIS

Two sequences of RHI profiles of the storm have been examined, one ten minutes prior to funnel sighting and one at the time of funnel sighting. The cloud was located at the optimum range for the RDR-1 radar and the profiles are relatively free from the distortion normal in RHI displays due to the compression of the horizontal axis. The vertical cross-sections revealed, in some detail, most of the characteristics found by radar analysis of a severe local storm: the hook echo, sloping overhang

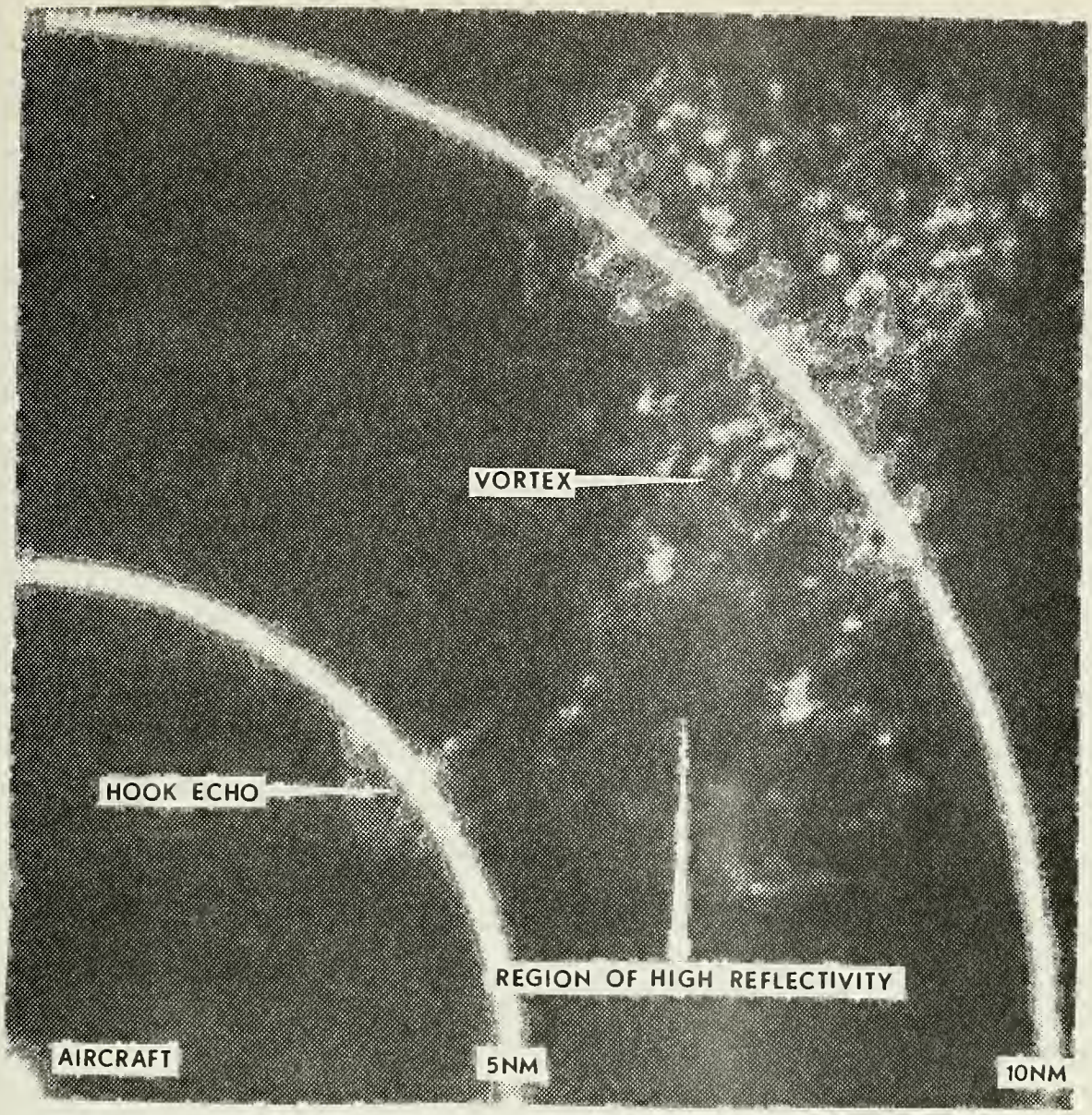

Figure 24. Enlarged view of profile 14 from Figure 23. Significant features are the horizontally-oriented vortex, the intensely reflective region below the vortex, the hook echo extending south from the cloud base and the cloud top extending beyond 60,000 feet.

and echo-free vault angling upshear and to the left with height. In addition, a horizontally-oriented vortex at high levels near the rear of the storm was noted. An explanation for the existence of this feature might be that it is a branch of the updraft that sustains the upshear portion of the anvil in the presence of eroding flow. The echo-free area just downwind of the vortex may indicate a region where the precipitation particles did not have time to grow to back-scattering size. This branch of circulation has been postulated in internal circulation models by Fujita (1965), Newton (1966) and Fankhauser (1971). Obviously, radars with displays that distort the vertical profile would tend to mask features such as the vortex discussed above.

The vertical extents of the highest echoes in the two sequences studied were in excess of 60,000 feet. This was considerably higher than the cloud tops shown by the WSR-57 vertical sequences. It would be expected that 3cm radar would show return to higher levels than 10cm radar because of the relative sizes of the back-scattering particles, but it has also been pointed out by experienced RDR-1 analysts (P. Black, NRHL, personal correspondence) that where intense echo intervenes, cloud tops are likely to be unreliable. It seems probable, then, that the actual tops were somewhere between 50,000 and 60,000 feet.

VI. CONCLUDING REMARKS

The mesoscale circulations inferred from analysis of aircraft measured winds fit existing models. The low-level inflow occurred along the right flank, a feature of both the Browning (1964) and Fankhauser (1971) models. The winds at 750mb displayed the characteristics of middle-level flow as is shown by the Browning and Fankhauser models, however, 750mb is a somewhat lower level than that indicated by Fankhauser (1971) for the entry of cool, dry middle-level air. Browning (1964) is less specific as to the level of middle-air inflow but it is also apparently higher than 750mb. The two vertical wind profiles did show that the veering between the surface and upper levels had taken place below the 750mb level. This would tend to place the 750mb level for this case in the lower part of the mid-level regime.

The interpretation of data from the three different radars (WSR-57, WP-101 and RDR-1) before, during and after the time of funnel sighting proved to be the most interesting part of this study. Unfortunately the RDR-1 profiles did not occur at the same times as the WSR-57 antenna tilt sequences.

The intense circulation that produced the funnel apparently lasted less than ten minutes (1630-1639 CST). The first WSR-57 sequence, it may be recalled, showed what appeared to be a vortex at 2° tilt, indicating substantial rotation at that time. The sighting of the funnel at 1637 would indicate substantial rotation extended through that time. The second WSR-57 vertical sequence revealed the vortex was no longer present at 1640. The disappearance of the low-level hook shortly thereafter substantiates this observation.

The RDR-1 RHI profiles of the upshear portion of the storm at the time of funnel sighting were the most difficult to interpret. The general impression was that the development of the funnel altered the shape of the storm considerably. This conclusion was not evident from the WSR-57 scope photographs but resulted from the comparison of the two RDR-1 sequences. Many interesting features were revealed by the RDR-1 sequences, including a hook echo, sloping overhang, echo-free vault, intensely reflective area around the vault and a high-level, horizontally-oriented vortex upshear of the vault.

A correlation of features between several radars was possible in some cases. The first involved the intensely reflective region which made up the core of the overhang in the second RDR-1 sequence. This corresponded well with the WSR-57 vertical sequence for the slightly earlier time, which showed the area of intense return extending along the right flank of the storm.

A comparison of the hook echoes from all three radars at the time of funnel sighting was also possible. All showed the hook was very well developed. The WP-101 hook echo shape was very similar to the WSR-57's with both revealing a narrow band of less intense return extending from the upshear edge to the center.

A third correlation, between the first WSR-57 vertical sequence and the second RDR-1 sequence was made. What was interpreted to be a circle of lesser intensity in the center of the hook region may be seen in the 1^{o} and 2^{o} tilt sections of the WSR-57 vertical sequence. This corresponded in position to the possible region of entry of the funnel into the storm mentioned in the discussion of the second sequence of RDR-1 profiles. The RDR-1 RHI profiles at the time of the funnel sighting are believed to be a unique sequence of photographs and are worthy of further study.

The fourth correlation concerns the vertical extent of the storm during the period the funnel is believed to have been present. If a comparison is made between the first and second WSR-57 vertical sequences and the first and second sequences of RDR-1 profiles, one can observe that the average cloud height decreased during the period between the respective sequences.

An overall view shows that most of the characteristics of this storm correlate well with the Browning (1964) model and the more detailed Fankhauser (1971) model. The region of possible funnel entry into the storm agreed with Bates' (The Severe Storms Research Group of Saint Louis University, 1970) depiction of funnel entry into the updraft, if his "flanking line" corresponds to the hook echo region of a severe storm.

VII. SUMMARY AND RECOMMENDATIONS

A. NAVIGATION

To achieve navigational accuracy approaching that deemed necessary by Fujita (1963) the flight track was broken into separate legs, each beginning with a fix. Although several TACAN stations including Oklahoma City and Ardmore were close, only five fixes were taken during the period that the aircraft was in the vicinity of the storm being investigated.

A fix (visual, TACAN) beginning and ending each straight and level leg would ensure better accuracy. Fixes should also be taken at times of significant events such as funnel or tornado sightings. In this study it was possible to generate additional fixes from WSR-57 radar IFF and skin "paints" on several long legs with excessive navigational errors. On the two legs where the aircraft was over the radar horizon of the NSSL radar, the end-of-leg errors were 1.8 and 2 nautical miles. No radar fixes were possible to further reduce these errors.

It is realized that the RFF aircraft navigational system was primarily intended for overwater use, but until the aircraft can be outfitted with either the relatively expensive inertial or inertial-Doppler navigational system, an interim solution to the navigational problem in areas where electronic fixes are continuously available may be feasible. If it were possible to digitize the TACAN readout and put it onto the data tape this would lend itself to data processing by computer. Better yet would be to have several TACANs, each tuned to a different station. There is room for such additional data on the existing one second data record used by the Research Flight Facility. The required information would be the TACAN

channel number and the range and bearing of the aircraft from that station. The range and bearing recorded at one second intervals would provide a "running fix" and, if the same was done for a second station, this would provide a backup.

B. FLIGHT SUMMARY

A more detailed flight log would be of great assistance to the investigator. In this case a more exact location of the funnel relative to the cloud would have been desirable. A detailed flight summary is especially helpful to the investigator when screening data.

C. LIBRARY OF TRACKS AND TIME-SPACE SERIES

Fujita (1970) has indicated the value of time-space series of cloud echoes in studying severe storms. If a library of these sequences could be accumulated by the National Severe Storms Laboratory or other agency then future statistical studies on storm tracks and development would be possible. In certain geographical regions there may be favored storm paths, whose existence would only be revealed by multiple storm observations.

APPENDIX A. SUPPLEMENTARY DATA AND INFORMATION

The tables included in Appendix A contain important information used in this study. Table IV lists the positions of the storm relative to NSSL at five minute intervals from 1430 to 1800 CST. Navigational data and meteorological parameters from the EMB-1 program as well as aircraft position information derived from the navigational data are shown in Table V. The results of Chapter IV were based on this data and information derived from it.

The following heading code is used for Table IV.

TCST - Central Standard Time

RPREC - Relative position of radar echo centroid from the National Severe Storms Laboratory's WSR-57 radar in NM.

The following heading code is used for Table V.

TCST - Central Standard Time

LAT - Latitude of aircraft from EMB-1 program.

LONG - Longitude of aircraft from EMB-1 program.

RNSSL - Aircraft position relative to the National Severe Storms Laboratory's WSR-57 radar in nautical miles. Computed from latitude-longitude.

RCEN - Aircraft position relative to the radar echo centroid in nautical miles.

WIND - Aircraft ambient wind from EMB-1 program (in knots).

RA - Height above terrain in feet.

P - Ambient pressure in millibars.

T - Ambient temperature in ^{o}C from vortex thermometer.

M/R - Mixing ratio in gm/kgm from infrared hygrometer.

RH - Relative humidity

* - Time of fix.

Table IV. Location of the radar echo centroid of the storm relative to NSSL at five minute intervals.

TCST	RPREC	TCST	RPREC
1430	184/61	1620	142/45.5
1435	184.5/58.5	1625	140/46
1440	184/58.5	1630	138/47
1445	183/57	1635	136/46.5
1450	181/55	1640	133.5/48
1455	179.5/54	1645	131/48
1500	178.5/52	1650	128/48
1505	176/51	1655	126.5/49.5
1510	173/48	1700	124/51
1515	171/47.5	1705	122/52
1520	168/46	1710	118.5/55
1525	168/45.5	1715	119/54
1530	166/45	1720	118/54.5
1535	164/44.5	1725	116.5/55
1540	162/45	1730	114.5/55.5
1545	159/44	1735	112.5/58.5
1550	157/44.5	1740	109.5/59.5
1555	154/44	1745	106/62
1600	151/45	1750	103.5/63.5
1605	149/45	1755	101.5/65
1610	148/45	1800	100/67
1615	144.5/46		

TCST	LAT	LONG	RNSSL	RCEN	WIND	RA	P	T	M/R	RH
1520	34 41.2	97 42.9	202/34	303/26	213/23	7700	726	5.7	3.6	45
1521	34 39.1	97 40.9	198/37	296/23	219/27	7812	725	5.3	4.3	55
1522	34 39.4	97 36.7	192/35	299/20	226/38	7781	725	5.2	4.1	53
1523	34 40.7	97 32.5	187/34	310/18	217/43	7866	723	3.7	5.7	81
1524	34 42.1	97 28.4	181/32	320/16	216/37	9045	693	0.6	6.1	104
1525	34 42.4	97 24.0	175/32	332/15	218/25	8856	699	1.4	5.9	97
1526	34 43.3	97 19.9	168/31	345/14	215/28	8870	702	3.3	6.0	96
1527	34 45.1	97 16.4	162/31	356/15	200/31	9702	680	0.6	5.6	100
1528	34 47.4	97 13.0	156/29	005/17	196/35	9838	676	0.4	4.7	84
1529	34 49.5	97 09.5	149/29	012/20	198/31	9963	672	-0.2	4.6	87
1530	34 51.6	97 05.8	142/29	020/22	191/32	10046	669	-0.4	4.1	77
1531	34 53.9	97 02.3	133/29	022/26	193/33	10009	669	-0.1	3.8	68
1532	34 56.1	96 58.7	127/30	025/29	195/30	10176	669	-0.1	3.4	61
1533	34 58.6	96 55.4	121/31	028/31	195/29	10173	668	0.0	2.9	53
1534	35 01.5	96 56.5	116/29	024/34	195/27	10016	669	-0.1	2.7	49
1535	34 59.2	96 58.6	122/28	022/31	203/15	9866	675	-0.2	2.7	49

Table V. Aircraft relative positions and important meteorological parameters.

TCST	LAT	LONG	RNSSL	RCEN	WIND	RA	P	T	M/R	RH
1536	34 56.0	97 0.6	129/29	021/27	195/18	9136	696	2.1	2.8	43
1537	34 53.6	97 03.8	137/29	016/23	182/16	8363	714	4.1	3.3	46
1538	34 51.4	97 07.1	144/28	010/20	179/18	7936	725	5.3	3.0	40
1539	34 49.3	97 10.4	151/28	002/18	183/25	7926	725	5.2	5.1	70
1540	34 47.6	97 13.4	157/29	353/16	193/25	7886	727	5.3	5.3	70
1541	34 45.6	97 16.1	162/30	341/15	199/20	7206	746	6.6	5.6	66
1542	34 43.6	97 19.2	167/31	326/14	195/17	6804	758	8.3	5.5	63
1543	34 42.1	97 22.4	173/32	312/15	203/16	6625	758	8.0	7.0	83
1544	34 40.7	97 25.6	177/34	301/16	230/30	6968	749	7.1	6.5	78
1545	34 40.3	97 28.6	182/34	295/18	232/27	7199	737	6.2	6.4	85
1546	34 39.7	97 31.7	186/35	289/21	225/26	7414	735	5.8	6.8	91
1547	34 37.2	97 32.5	187/37	-	226/27	6570	758	7.4	7.2	83
1548	34 35.4	97 29.3	182/39	-	222/33	6190	775	9.5	7.2	76
1549	34 37.1	97 25.1	177/37	-	220/38	5827	783	10.8	6.2	62
1550	34 40.1	97 25.6	177/34	-	220/37	5292	797	11.0	8.5	81
1551	34 39.2	97 28.1	182/36	282/20	217/27	5530	789	11.5	8.4	84

Table V. Aircraft relative positions and important meteorological parameters.

TCST	LAT	LONG	RNSSL	RCEN	WIND	RA	P	T	M/R	RH
1552	34 36.8	97 27.8	181/37	279/19	223/30	6227	773	11.0	7.2	78
1553	34 34.3	97 26.3	179/40	270/18	230/33	6794	758	9.3	4.6	50
1554	34 31.8	97 24.4	177/43	261/17	228/32	6981	751	8.4	4.9	56
1555	34 28.9	97 22.6	175/46	250/17	222/31	6880	752	8.3	5.5	62
1556	34 25.9	97 20.8	174/49	239/17	224/30	6852	753	8.3	4.5	50
1557	34 23.0	97 18.9	172/52	228/18	226/28	6954	753	8.3	6.1	70
1558	34 23.2	97 14.7	169/52	221/16	229/31	6851	753	8.3	6.4	73
1559*	34 23.0	97 10.9	165/53	212/15	232/39	6686	755	8.8	5.9	66
1600	34 22.8	97 06.3	161/55	195/13	221/43	6695	753	8.1	7.0	83
1601	34 22.3	97 01.8	158/56	183/14	210/39	7107	753	8.3	5.7	67
1602	34 22.4	96 57.3	155/58	170/14	202/37	6919	752	8.3	5.1	59
1603	34 22.5	96 52.8	151/59	156/15	203/34	6889	752	8.3	5.5	63
1604	34 22.5	96 48.4	148/61	146/17	204/32	6970	752	8.4	5.5	63
1605	34 22.5	96 44.0	145/63	137/19	199/26	6990	752	8.3	4.4	50
1606	34 22.4	96 39.5	143/65	132/21	209/26	6980	753	9.0	3.6	39
1607	34 21.4	96 35.8	142/68	131/25	209/26	7080	754	9.5	5.4	62

Table V. Aircraft relative positions and important meterological parameters.

TCST	LAT	LONG	RNSSL	RCEN	WIND	RA	P	T	M/R	RH
1608	34 19.5	96 38.0	143/68	136/24	200/24	7067	755	9.4	6.3	72
1609	34 20.0	96 42.0	145/66	142/22	196/26	7072	753	8.9	3.6	39
1610	34 20.6	96 46.0	148/64	152/19	192/24	6963	755	8.8	5.8	64
1611	34 21.2	96 50.0	150/61	162/17	193/28	6849	754	8.5	5.2	57
1612	34 22.1	96 53.9	152/59	172/16	202/28	6994	753	8.6	3.4	37
1613	34 23.0	96 57.1	154/57	184/15	208/33	6877	752	8.5	5.8	65
1614	34 24.0	97 01.6	157/55	201/15	223/35	7205	752	8.3	5.9	64
1615	34 25.0	97 05.4	160/52	214/16	234/27	6977	752	8.3	7.1	82
1616	34 25.7	97 09.1	163/51	225/17	225/21	6763	752	7.3	7.5	89
1617	34 26.0	97 12.9	166/50	232/20	218/20	6571	755	7.8	7.6	90
1618	34 24.0	97 12.8	167/52	228/21	231/25	6610	755	8.3	6.7	77
1619*	34 23.5	97 09.0	163/52	222/20	232/26	6114	772	8.5	8.1	85
1620	34 20.6	97 08.5	164/56	215/22	223/22	5186	802	11.8	8.1	74
1621	34 20.8	97 11.7	166/55	220/24	223/22	4262	827	13.8	9.5	79
1622	34 23.2	97 09.8	164/53	222/22	208/25	3648	842	14.8	10.7	84
1623	34 23.9	97 05.6	160/54	216/20	196/27	3171	863	16.5	12.2	91

Table V. Aircraft relative positions and important meteorological parameters.

TCST	LAT	LONG	RNSSL	RCEN	WIND	RA	P	T	M/R	RH
1624	34 24.6	97 01.5	157/54	209/17	198/33	2928	875	17.5	11.7	83
1625	34 25.5	96 57.5	153/55	201/16	185/38	2655	880	17.9	13.0	95
1626*	34 28.1	96 53.7	149/56	193/12	165/38	2128	890	17.8	13.7	99
1627	34 29.2	96 50.0	146/55	181/11	146/31	2111	889	17.8	13.7	100
1628	34 30.0	96 46.5	143/56	170/11	136/25	1525	908	17.8	13.8	99
1629	34 29.9	96 43.0	140/58	157/12	144/23	1609	906	17.9	13.9	97
1630	34 30.0	96 39.7	138/60	147/13	157/25	1724	906	18.0	13.6	97
1631	34 30.1	96 36.0	136/61	139/14	157/23	1722	905	17.6	13.8	99
1632	34 29.5	96 32.8	135/64	134/17	158/22	1752	908	17.8	13.7	100
1633	34 28.4	96 35.6	137/63	142/16	142/24	1784	906	18.0	13.6	94
1634	34 28.7	96 39.7	139/61	155/14	132/26	1721	905	18.1	13.7	100
1635	34 28.9	96 44.0	142/58	170/13	134/27	1619	905	18.0	13.8	99
1636	34 28.6	96 48.1	145/56	188/13	141/28	1658	904	18.0	14.0	99
1637	34 28.2	96 52.3	148/55	200/15	158/29	1728	904	18.5	13.8	93
1638	34 27.8	96 56.5	151/53	213/17	157/25	1762	903	19.1	13.3	89
1639	34 28.1	97 00.6	154/51	222/19	156/20	2051	902	19.4	13.3	86

Table V. Aircraft relative positions and important meteorological parameters.

TCST	LAT	LONG	RNSSL	RCEN	WIND	RA	P	T	M/R	RH
1640*	34 27.0	97 05.7	158/52	229/23	156/20	2050	903	19.4	13.5	86
1641	34 25.8	97 03.1	158/53	223/23	175/24	1838	906	19.8	13.5	88
1642	34 26.5	96 59.5	154/53	219/21	176/29	1947	904	19.5	12.9	83
1643	34 27.4	96 55.6	151/54	213/19	175/29	1455	916	20.1	13.5	84
1644	34 28.1	96 52.0	148/55	207/17	177/28	1692	905	19.1	14.0	95
1645	34 28.8	96 48.4	145/56	200/15	168/28	1697	905	18.0	14.1	101
1646	34 28.8	96 44.9	142/58	190/15	163/30	1669	904	17.7	14.1	102
1647	34 29.0	96 41.2	140/59	180/14	164/27	1709	904	17.8	13.9	102
1648	34 28.9	96 37.6	138/62	170/15	156/23	1812	904	18.1	13.0	88
1649	34 28.6	96 34.0	136/64	160/16	151/20	1905	904	17.0	13.9	107
1650	34 29.2	96 30.5	134/65	153/17	151/21	1836	911	17.8	13.8	100
1651	34 31.0	96 27.5	131/66	145/17	156/26	1836	911	17.8	13.6	98
1652	34 33.1	96 24.7	128/67	134/16	156/28	2006	912	17.8	13.5	96
1653	34 35.2	96 21.9	126/67	125/17	152/27	1779	917	17.7	13.3	96
1654	34 37.3	96 19.0	123/68	116/18	155/28	1658	919	18.0	13.4	96
1655	34 39.4	96 16.2	121/68	108/18	156/29	1677	920	18.3	13.1	92

Table V. Aircraft relative positions and important meteorological parameters.

TCST	LAT	LONG	RNSSL	RCEN	WIND	RA	P	T	M/R	RH
1656	34 41.5	96 13.5	118/69	101/19	157/30	1737	921	18.3	13.0	91
1657	34 40.5	96 11.5	118/71	103/21	155/29	1566	924	18.5	12.9	90
1658	34 39.3	96 14.6	120/70	110/18	134/22	1622	921	18.3	13.0	91
1659	34 38.0	96 18.0	122/68	118/16	130/22	1561	921	18.4	13.0	92
1700	34 36.8	96 21.2	124/66	130/14	132/21	1656	921	18.2	13.2	93
1701	34 35.2	96 24.1	127/66	142/14	125/18	1617	921	18.1	13.4	95
1702	34 33.6	96 27.2	129/64	157/14	133/20	1615	921	18.3	13.4	96
1703	34 32.0	96 30.2	132/64	170/15	133/20	1645	920	18.6	13.6	93
1704	34 30.4	96 33.2	134/68	182/16	122/19	1276	921	18.4	13.8	96
1705	34 28.9	96 36.1	137/62	191/19	137/19	1673	909	17.8	13.9	99
1706	34 28.0	96 39.1	139/61	199/21	162/26	2053	895	17.7	13.4	96
1707	34 28.7	96 42.4	141/59	208/22	183/29	2935	866	16.4	12.9	100
1708	34 29.2	96 45.5	142/57	215/23	190/31	3514	847	15.8	11.0	86
1709*	34 31.0	96 50.0	143/54	226/25	187/32	4227	824	13.9	10.5	92
1710	34 32.4	96 53.0	146/51	232/27	191/31	4919	805	11.6	10.9	103
1711	34 30.7	96 53.9	148/52	229/29	203/28	5491	789	11.1	7.9	78

Table V. Aircraft positions and important meteorological parameters.

TCST	LAT	LONG	RNSSL	RCEN	WIND	RA	P	T	M/R	RH
1712	34 28.6	96 51.8	147/54	225/29	227/28	6168	770	10.3	6.8	70
1713	34 26.4	96 52.3	149/56	222/31	230/24	6933	751	9.1	6.0	68
1714	34 24.8	96 54.5	151/56	222/33	220/24	7505	735	7.4	6.1	76
1715	34 23.9	96 57.5	154/56	225/36	228/22	8118	721	5.6	6.5	89
1716	34 23.2	97 00.5	157/56	227/38	222/30	8625	709	4.4	4.6	62
1717	34 23.6	97 04.0	159/54	230/40	223/26	9608	686	3.2	4.8	76
1718	34 23.6	97 07.0	162/53	232/42	235/25	10020	667	0.4	4.0	72
1719*	34 24.0	97 10.0	165/52	234/44	238/32	10349	658	-0.6	3.7	72
1720	34 23.6	97 13.1	167/52	236/46	239/39	11293	634	-2.6	3.3	72

Table V. Aircraft positions and important meteorological parameters.

LIST OF REFERENCES

1. Browning, K.A., and F.H. Ludlam, 1962: Airflow in convective storms. Quart, J. R. Meteor. Soc., 88, 117-135.

2. _____, 1964: Airflow and precipitation trajectories within severe local storms which travel to the right of the winds. Journal of the Atmospheric Sciences, 21, 634-639.

3. _____, and T. Fujita, 1965: A family outbreak of severe local storms in Oklahoma on 26 May 1963, Part I. Air Force Cambridge Research Laboratories Special Reports, No. 32, 1-346.

4. _____, and R.J. Donaldson, Jr., 1963: Airflow and structure of a tornadic storm. Journal of the Atmospheric Sciences, 20, 533-545.

5. Donaldson, R.J., Jr., 1965: Methods of identifying severe thunderstorms by radar: a guide and bibliography. Bulletin of the American Meteorological Society, 46, 174-193.

6. Fankhauser, J.C., 1964: On the motion and predictability of convective systems as related to the upper winds in a case of small turning of wind with height. National Severe Storms Project Report No. 21, 1-36.

7. _____, 1971: Thunderstorm-environment interactions determined from aircraft and radar observations. Monthly Weather Review, 99, 171-192.

8. Friedman, H.A., M.R. Ahrens and H.W. Davis, 1969: The ESSA Research Flight Facility: data processing procedures. Technical Report ERL 132-RFF 2, 1-49.

9. Fujita, T., 1963: Analysis of selected aircraft data from NSSP operations, 1962. U.S. Weather Bureau Severe Storms Project Number 16, 1-17.

10. _____, 1965: Formation and steering mechanisms of tornado cyclones and associated hook echoes. Monthly Weather Review, 93, 67-78.

11. _____, and H. Grandoso, 1968: Split of a thunderstorm into anticyclonic and cyclonic storms and their motion as determined from numerical model experiments. Journal of the Atmospheric Sciences, 25, 416-439.

12. _____, D.L. Bradbury and C.F. Van Thullenar, 1970: Palm Sunday tornadoes of April 11, 1965. Monthly Weather Review, 98, 29-69.

13. Hamilton, R.E., 1969: A review of use of radar in detection of tornadoes and hail. ESSA Technical Memorandum WBTM-ER-34, 1-59.

14. Kessler, E., 1970: Thunderstorms over Oklahoma - 22 June 1969. Weatherwise, April, 56-69.

15. Newton, C.W. and J.C. Fankhauser, 1964: On the movements of convective storms, with emphasis on size discrimination in relation to water-budget requirements. Journal of Applied Meteorology, 3, 651-668.

16. _____, 1966: Circulations in large sheared cumulonimbus. Tellus, XVIII(1966), 4, 699-712.

17. Reber, C.M. and H.A. Friedman, 1964: Manual of meteorological instrumentation and data processing. Research Flight Facility, U.S. Weather Bureau.

18. The Severe Storms Research Group of Saint Louis University, 1970: F.C. Bates conceptual thoughts on severe thunderstorms. Bulletin of the American Meteorological Society, 51, 481-487.

INITIAL DISTRIBUTION LIST

		No. Copies
1.	Defense Documentation Center Cameron Station Alexandria, Virginia 22314	2
2.	Library, Code 0212 Naval Postgraduate School Monterey, California 93940	2
3.	Asst Professor R.L. Alberty, Code 51 Al Department of Meteorology Naval Postgraduate School Monterey, California 93940	10
4.	Lt. C.E. Horswell, USN U.S. Fleet Weather Central Box 12 COMNAVMARIANAS FPO San Francisco 96630	5
5.	Assoc Professor R.L. Elsberry, Code 51 Es Department of Meteorology Naval Postgraduate School Monterey, California 93940	1
6.	Professor R.J. Renard, Code 51 Rd Department of Meteorology Naval Postgraduate School Monterey, California 93940	1
7.	Department of Meteorology Naval Postgraduate School Monterey, California 93940	2
8.	Naval Weather Service Command Naval Weather Service Headquarters Washington Navy Yard Washington, D.C. 20390	1
9.	Peter G. Black, Research Meteorologist National Hurricane Research Laboratory P.O. Box 8265, University of Miami Beach Coral Gables, Florida 33124	1
10.	Jerome W. Nickerson Head, Special Studies Division ENVPREDRSCHFAC, Naval Postgraduate School Monterey, California 93940	1

UNCLASSIFIED

Security Classification

DOCUMENT CONTROL DATA - R & D

(Security classification of title, body of abstract and indexing annotation must be entered when the overall report is classified)

1. ORIGINATING ACTIVITY (Corporate author)

Naval Postgraduate School
Monterey, California 93940

2a. REPORT SECURITY CLASSIFICATION

Unclassified

2b. GROUP

3. REPORT TITLE

A Study of a Severe Local Storm of 22 April 1971

4. DESCRIPTIVE NOTES (Type of report and inclusive dates)

Master's Thesis; September 1972

5. AUTHOR(S) (First name, middle initial, last name)

Charles E. Horswell

6. REPORT DATE	7a. TOTAL NO. OF PAGES	7b. NO. OF REFS
September 1972	71	18

8a. CONTRACT OR GRANT NO.	9a. ORIGINATOR'S REPORT NUMBER(S)
b. PROJECT NO.	
c.	9b. OTHER REPORT NO(S) (Any other numbers that may be assigned this report)
d.	

10. DISTRIBUTION STATEMENT

Approved for public release; distribution unlimited.

11. SUPPLEMENTARY NOTES	12. SPONSORING MILITARY ACTIVITY
	Naval Postgraduate School Monterey, California 93940

13. ABSTRACT

A study was made of a severe storm that occurred on 22 April 1971 southeast of Norman, Oklahoma. The life cycle of the storm from origin, through mature stage, to eventual incorporation into a squall line was analyzed. The cell displayed all of the characteristics of a severe local storm, including a hook echo, echo-free vault, sloping overhang, funnel and movement 20° to the right of the mean tropospheric wind. Mesoscale circulations at low and middle levels during the severe stage were revealed by aircraft measured winds. Aircraft meteorological parameter measurements showed the vertical structure and extent of the low-level moist layer. Three-dimensional storm structure at the time a funnel was sighted was inferred from WSR-57 radar antenna tilt sequences and airborne RDR-1 radar RHI profiles.

DD FORM 1 NOV 68 1473 (PAGE 1)

S/N 0101-807-6811

UNCLASSIFIED

Security Classification

A-31408

14. KEY WORDS	LINK A		LINK B		LINK C	
	ROLE	WT	ROLE	WT	ROLE	WT
Severe local storm						
Funnel sighting						
Squall line						
Radar profiles						
Hook echo						

Thesis
H8038
c.1

Horswell.

139043

A study of a severe local storm of 22 April 1971.